Università degli Studi di Padova

Dipartimento di Matematica "Tullio Levi-Civita"

Corso di Laurea in Matematica

Fast-Slow Systems and Bifurcations in Neuroscience

Relatore: Prof. Giancarlo Benettin
Correlatore: Prof. Robert S. MacKay
Laureando: Francesco Morabito
Matricola: 1120496
Data Sessione di Laurea: 28 Settembre 2018

Contents

Introduction

While this document contains no original notion nor new approach to the subject, I think it can give the reader a good overview of how various the behaviours of biological systems may be, and of how the mathematics of Dynamical Systems can predict unusual phenomena. This dissertation is opened with a (very) short introduction to the biological setting, so that the reader can make a sense of the content which goes beyond the mathematics involved in the description, for the sake of completeness and to (hopefully) rise their interest in the matter with a simplified exposition by somebody who is not a biologist and tried to analyse a biology book with the eyes of a mathematician-to-be.
In the second chapter we introduce the Hodgkin-Huxley and the FitzHugh-Nagumo systems; if the former was one of the first attempts to mathematically model how an action potential (i.e. the neuronal impulse, but see Chapter 1) in neurons, in the derivation and the analysis of the latter we use one of the two main recurrent ideas of this text: fast-slow systems. This is a very peculiar kind of systems of ODEs where variables change at different rates but can be distinguished in "fast" and "slow" variables: this structure will be used twice, by FitzHugh to derive his model and by us to perform the analysis of *canards*, based on a theorem by Fenichel. Canards are a special kind of solutions for the system which are completely unexpected, the reader will see why in Chapter 2, and fundamental to the study of the study we shall lead: we will not define the meaning of the following words here, as they will be defined in the relevant parts of the document, but the presence of canards implies the absence of a voltage threshold for the generation of the action potential, and this is not what one would expect to see as it appears to be the opposite of what can be seen in experiments.
Already in this chapter we can see a simple example of bifurcation: given the dimensionality of the problem we can apply phase-plane methods, in this case the *Poincaré-Bendixson theorem* to prove the generation, while a parameter of the system varies smoothly, of an attractive limit cycle from a stable equilibrium which loses stability.
In Chapter 3 we will analyse the Morris-Lecar model: after performing a dimensional reduction (one can already find its motivations in the original paper) applying a Theorem by Tikhonov, we will start showing, helping ourselves with simulations in MATLAB, the incredible variety of phenomena which the model can give rise to, with little variations of parameters which can be in fact experimentally manipulated. The first study will involve just one bifurcation parameters, but then we will always work with two bifurcation parameters simultaneously, describing a variety of qualitative behaviours, and their transitions, of the solutions, sometimes with really bizarre conclusions.

After this short description of the material contained here, the reader will have understood the reason of the title: fast-slow structures and bifurcations have been used and investigated thoroughly in this document, providing at the very least motivation to study mathematically these ideas, and more optimistically an intuition of the power of such methods when it comes to deal with complex problems and nonlinearity.

So far I have described what I wrote and why I wrote it, now I need to state how I wrote it. This dissertation has been almost completely (apart from this introduction and some minor changes through the text) written during my Erasmus+ mobility at the University of Warwick, Coventry, UK, under Professor Robert S. MacKay, FRS FInstP FIMA, whom I wish to thank here for his constant help and patience when I went to him full of doubts and required explanations, or when I needed to discuss what to study next, or just wanted to talk a little bit. I am very grateful for having the possibility of knowing and working with him.

Chapter 1

Biological overview

1.1 Anatomy of a neuron

The neuron is, as it is well known, one of the kind of cells which a brain is made up of: neuronal cells fulfil a great variety of functions and their anatomic features reflect their specific functions. Nevertheless, it is possible to recognise a general scheme to which the anatomy of a neuron must obey. Generally speaking[1], the four constitutive parts of a neuron are the **dendrites**, the **cell body** (also called *soma* or *perikaryon*), the **axon** and a **synaptic termination**.
Dendrites are extremities of the cell which collect information from other neurons: they provide a large receiving area creating a ramified structure with receptors at the end of each branch. The form of the dendritic tree can be used to infer the role of the single neuron and the type of information it receives[2]. The shape of the dendritic tree is maintained by both intercellular superficial interactions and intracellular structural devices.
The perikaryon contains the cell nucleus and cytoplasmatic organelles, in particular levels of protein synthesis in neurons need to be kept high: this process involves a quantity of steps which go from the transcription of the DNA into mRNA to the actual synthesis. It is remarkable that the organisation of the Rough Endoplasmatic Reticulum (RER), a cytoplasmatic organelle necessary to the protein synthesis, is peculiar in neurons: stacks of RER are interposed with arrays of free ribosomes, and the functional important of such a structure is currently unknown.
The axon is a wire through which the information flows, from the perikaryon to other neurons: this information is transmitted as an electrical stimulus, called **action potential**. This is primarily generated at the axon hillock, the area of connection between the axon and the perikaryon: the process of generation of the action potential is the main topic of this dissertation, and will be examined in greater detail in the following chapters.
Synapses are the places where two neurons connect and exchange information. They are made up of three parts: a pre-synaptic element, a cleft and a post-

[1] What follows is referring to multipolar neurons, the most common kind of neuronal cell.
[2] As reported in [13], page 42, the width of the dendritic arbor can be used for example to infer how large the pool of afferents is: a pyramidal neuron, an excitatory neuron whose function is to make distant contacts, will have a wider dendritic tree than a neuron whose afferents belong in a particular cortical layer.

synaptic element. Seen in cross-section, the first and the third part look like two parallel segments, separated by the cleft, which is a very narrow strip of empty space. The presynaptic element belongs in the neuron which transmits the information, at the very end of its axon[3]; this area contains the synaptic vesicles which, when stimulated by an action potential, release neurotransmitters, biomolecules which spread across the cleft and reach the post-synaptic element. The post-synaptic element belongs in a dendrite of a neuron and receives the information which will be processed in the perikaryon, and in some cases transmitted again through the axon.

1.2 The action potential

As mentioned in the previous section, the action potential is an electrical stimulus which is used to transmit encoded information from one neuron to another. In this section we shall describe the setting necessary for the generation of the action potential, what kind of objects is involved and how. This will lead to the next chapter, describing the Fitzhugh-Nagumo model.

1.2.1 Membrane potential

Membranes in neurons carry out the function of creating a potential difference between the inside and the outside of the cell. This aim is achieved by regulating the concentrations of several ions, among which we can mention Na^+, Ca^{2+}, K^+, Cl^-, inside the neuron. The plasma membrane contains pores, called **ionic channels**, which let specific ions pass: these therefore tend to reduce the concentration gradient between the two sides of the membrane, and this results in changes in the electric field. At some point the voltage is such that, because of electrostatic forces and thermodynamics laws, the probabilities of one ion getting in or out the cell are the same: we call this **equilibrium potential**. By definition the equilibrium potential can be different for each kind of ion, and the **resting potential** of a neuron, i.e. the voltage of a cell at rest, will be a weighted average of the equilibrium potentials. When the cell is at resting potential, ions flow spontaneously through the ionic channels according to their concentration gradients, as the voltage is not an equilibrium for any ion, and the cell can contrast this flux thanks to the work of **membrane proteins**, which spend energy in order to move the ions against their concentration gradients, and to keep the voltage stable at the resting potential.
Resting potentials are different depending on the different kind of neurons, but they are always negative (i. e. positive ions tend to flow from the outside to the inside), and on average around -60 mV.

1.2.2 Action potential

An action potential is a rapid increase followed by a decrease in the membrane potential of the axon. The stimulus propagates then along the nerve, towards the synaptic terminations, maintaining its shape.
In general the action potential is generated in the axon hillock (the juncture

[3]This statement might be overly simplified and imprecise, but it will suffice for the purposes of this dissertation.

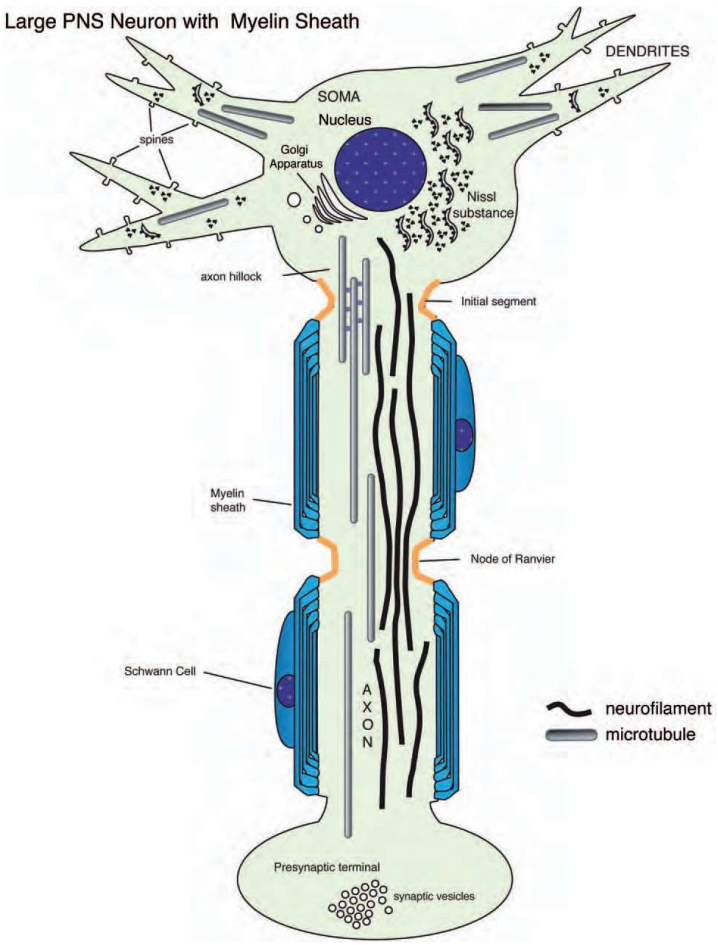

Figure 1.1: The structure of a neuron in the Peripheral Nervous System, [13], page 61.

between axon and perikaryon) by a sudden increase in the conductance of the membrane to the Na^+ ions. Meanwhile K^+ ions are pushed out of the cell: overall we have two currents, in the following I_{Na}, inwards, and I_K, outwards. There are some fundamental differences between the two: I_{Na} is faster in getting triggered and is inactivated when the voltage reaches 0 mV, while I_K is slower in activating, but also is sustained while the membrane potential is positive. A hypothesis about this process by Hodgkin and Huxley states that channels for K^+ ions are open in case of a non zero voltage, while the behaviour of Na^+ is more complex: they appear to have two processes triggered by voltage, activation-deactivation and deactivation-inactivation. By "**activation**"we mean the state in which Na^+ channels do not prevent the flux of ions. The phase of **inactivation** corresponds to a closed state of the Na^+ channels when the stimulus is still present. **Deactivation** is a closed state of the channels after the stimulus has vanished.
We shall now propose the description by Hodgkin and Huxley for the steps involved in an action potential, as reported in [13]. A first depolarisation increases the number of the activated sodium channels, to create a flux of positive sodium ions from the outside to the inside of the cell. When a certain potential, called **potential threshold**[4], is reached the flux of ions triggers a positive feedback loop, depolarising consistently the membrane, taking the potential towards the voltage for the equilibrium of the sodium ions (defined in the previous section). With the increase of the quantity of sodium inside the axon, however, the channels deactivate, and the flow is slowed. Meanwhile the channels for the potassium ions open, and when the outflow of potassium ions starts dominating the voltage reaches its positive peak (which can reach 40 mV) and starts falling. As the interruption of I_K is delayed, the membrane gets a negative voltage which is in absolute value greater than the resting potential: this phase is called **after-hyperpolarisation**, and it covers a period of time in which the axon cannot generate or transport an action potential, and we speak of the **refractory period**. Now channels for sodium ions are activated again and channels for potassium are closed: the axon is ready for the generation of another action potential.
As mentioned in the previous section, the action potential propagates along the axon, both towards the synaptic terminations and the perikaryon: when it reaches the synapses it causes the release of neurotransmitters, and the component which passes through the body and gets to the dendrites acts as a signal for the regulation of intracellular processes. It surely is important therefore to prevent reverberations and oscillations of the action potential: this function is performed by the refractory period above, as in that phase a greater depolarisation is required for a new action potential, due to the inactivated sodium channels and the steady outwards-bound potassium current.

[4] Usually this voltage is -55 mV.

Chapter 2

The Fitzhugh-Nagumo model

In this chapter we shall first construct the Hodgkin-Huxley model for the generation of the action potential, of which Fitzhugh-Nagumo is a mathematical simplification, in order to get a better understanding of the biological meanings of the mathematical results.

2.1 The Hodgkin-Huxley model

This model was first proposed in [5], and it was constructed thanks to the authors' studies about the giant squid axon. In the following we shall denote, as before, the sodium and the potassium currents as I_{Na} and I_K respectively. We shall consider a small leakage current, I_l, whose presence is due to the movement of other ions. E_r will be the resting potential, E_{Na} and E_K the equilibrium potentials for sodium and potassium respectively. g_{Na} and g_K will be their respective conductances, and g_l will stand for an average conductance to other ions. To introduce the first equation we need to define the total current, $I(t)$, positive if directed inwards, the total ionic current $I_i(t) = (I_{Na}+I_K+I_l)(t)$, again positive if inwards, the displacement of the membrane potential from the resting value $V(t) = E - E(t)$ (with this definition $V < 0$ during the depolarisation phase) and the capacity of the membrane per unit area C_M: this last quantity is assumed constant. Hodgkin and Huxley proposed the following equation:

$$I = C_M \dot{V} + I_i \tag{2.1}$$

where $\dot{V}$ is the temporal derivative of V. The validity of this equation is justified by previous studies of the authors. However, Hodgkin and Huxley recognise that this law does not consider any dielectric loss of the membrane, but the error introduced in this way does not appear to be very large.
Now we need to express the total current in terms of the voltage $V(t)$. For $j \in \{\text{Na, l, K}\}$ we have

$$I_j = g_j(E(t) - E_j) = g_j(V(t) - V_j)$$

where $V(t) = E(t) - E_r$ and $V_j = E_j - E_r$. The conductances are not constant, and we need further equations to completely describe the system.

The potassium conductance By data from previous experiments, Hodgkin and Huxley inferred that the best assumption, in terms of simplicity and effectiveness, was that g_K was proportional to the fourth power of a certain quantity, that we shall call $n \in [0,1]$, which followed a first order ordinary differential equation. It turned out that the following relations were a good description:

$$g_K = \bar{g}_K n^4$$

$$\dot{n} = \alpha_n(1-n) - \beta_n n \tag{2.2}$$

where $\bar{g}_K$ is constant, while α_n and β_n are functions of voltage, but not directly of time. The dimensions are as follows:

$$[\bar{g}_K] = \frac{\mathrm{S}}{\mathrm{cm}^2}$$
$$[\alpha_n] = [\beta_n] = 10^3 \mathrm{s}^{-1}$$

Hodgkin and Huxley suggest the following interpretation for the variable n: they proposed that K^+ ions could get through the membrane if and only if four particles (of which we do not know anything, they are not even required to be of the same kind) were found in a specific configuration. In this case n would be a probability of finding one of the our particles in the proper place. In particular it would seem that positions of the particles are mutually independent (given the fourth power in the equation). Note that n might be some sort of statistic approximation we can make and have no significance for small numbers of particles. In this interpretation α_n assume the role of the rate with which ions flow from the outside to the inside and β_n of the rate for the opposite movement. By the discussion in the previous chapter one should expect α_n to decrease and β_n to increase during the depolarisation of the membrane.

The sodium conductance Hodgkin and Huxley found two methods to properly describe the more complex behaviour of the sodium conductance: either using a second-order ODE with one variable or using a first-order ODE with two variables, each of which following a first-order ODE. The latter method was preferred, as it had a simpler application to the experimental results[1]. The formal laws they inferred are similar to the ones used for the case of the potassium:

$$g_{Na} = m^3 h \bar{g}_{Na}$$

$$\dot{m} = \alpha_m(1-m) - \beta_m m \tag{2.3}$$

$$\dot{h} = \alpha_h(1-h) - \beta_h h \tag{2.4}$$

The physical meaning can be given in an analogous way as well: we may assume that the transfer of sodium from the outside to the inside of the cell is possible if and only if there are three similar particles which are in a certain position, and a fourth one is not blocking the channel. m in this interpretation would be the probability of finding a particle that lets sodium flow in the correct position, and h the probability of a blocking molecule not to be in the right site. Dimensions and assumptions on m and h are the same made for n, and α_j, β_j for $j \in \{m, h\}$ are again the rates of transfer.

[1] See [5], page 512.

The whole description Plugging the expressions for the conductances into (2.1) we now have the complete Hodgkin-Huxley quantitative description of the generation of the action potential:

$$\begin{cases} I &= C_M\dot{V} + \bar{g}_K n^4(V - V_K) + m^3 h\bar{g}_{Na}(V - V_{Na}) + g_l(V - V_l) \\ \dot{n} &= \alpha_n(1-n) - \beta_n n \\ \dot{m} &= \alpha_m(1-m) - \beta_m m \\ \dot{h} &= \alpha_h(1-h) - \beta_h h \end{cases}$$

where we assumed the conductance for the leakage current to be constant. It is evident that an analytic study of this system would be fairly complicated. In the next section we shall introduce one of the main topics of this dissertation.

2.2 FitzHugh-Nagumo: the construction

This model (FN) was first proposed by R. Fitzhugh in [2]. It consists of a simplification of the Hodgkin-Huxley model, meant to make the analysis of the qualitative behaviour of solutions for Hodgkin-Huxley easier, without losing any important dynamical behaviour regime but sacrificing adherence to biological data. The ODEs describing the system are as follows:

$$\begin{cases} \dot{u} &= c\left(w + u - \frac{u^3}{3} + z\right) \\ \dot{w} &= -\frac{(u - a + bw)}{c} \end{cases}$$

with the following conditions on the parameters:

$$\begin{cases} 1 - \frac{2b}{3} < a < 1 \\ 0 < b < 1 \\ b < c^2 \\ c > 0 \end{cases}$$

where z is a function of time, corresponding to an electrical stimulus. The reasons for the constraints will be later analysed.
What is immediately noticed is that in FN we have only two variables, while in HH the number of degrees of freedom is four (recall that the variables describing the system are V, m, n, h). To understand how the variables are eliminated we need a quick analysis of the HH model, found in [4].

2.2.1 HH reduced systems

The key idea here is that we can split the four variables of the HH model into two pairs: over a same (small enough) interval of time V and m can change noticeably, whereas h and n can not. With this observation we are allowed to conclude that, fixing h and n to a constant value, we can first study the dynamics of the pair (V, m), to reinsert later h and n into the system. The following is a short and heuristic description of the derivation of the FN model, rigorous justification and precise numerical simulations can be found in [2].

The (V, m) plane Set n and h constant and assume for simplicity $I = 0$. With elementary calculations we can solve the differential equation involving m for any fixed voltage V (recall that the parameters α_m, β_m are functions of the voltage). The solution is the following:

$$m(t) = m_\infty(V) - (m_\infty(V) - m_0) \exp\left(-\frac{t}{\tau_m}\right) \tag{2.5}$$

where $m_\infty(V) = \lim_{t\to\infty} m(t) = \frac{\alpha_m(V)}{\alpha_m(V)+\beta_m(V)}$, $m_0 = m_\infty(0)$, $\tau_m = \frac{1}{(\alpha_m+\beta_m)(V)}$. To perform numerical simulations it is therefore necessary to find the functions describing α_m, β_m. Hodgkin and Huxley in [5] found the following expressions:

$$\alpha_m = \frac{0.1(V+25)}{\exp\left(\frac{V+25}{10} - 1\right)} \tag{2.6}$$

$$\beta_m = 4\exp\left(\frac{V}{18}\right) \tag{2.7}$$

where V is measured in mV.
We now want to plot in the phase plane (V, m) the trajectories of the reduced system. To do so we need to choose the values for h and n: we shall fix them at their resting values, which are h_∞ and n_∞. These are given by the expressions:

$$h_\infty(V) = \frac{\alpha_h(V)}{\alpha_h(V) + \beta_h(V)}$$

$$n_\infty(V) = \frac{\alpha_n(V)}{\alpha_n(V) + \beta_n(V)}$$

which were derived with a similar procedure as the one used above. The projection on the (V, m) plane of the system is therefore determined by the following system of ODEs:

$$\begin{cases} \dot{V} &= -\bar{g}_K n_\infty^4 (V - V_K) - m^3 h_\infty \bar{g}_{Na}(V - V_{Na}) - g_l(V - V_l) \\ \dot{m} &= \alpha_m(1-m) - \beta_m m \end{cases}$$

where we set $C_M = 1$, as this is the experimental value found for it. Plotting the nullclines $\{\dot{V} = 0\}$ and $\{\dot{m} = 0\}$ we see that we have three intersections of the curves, two of which are close to the origin: see figures 2.1 (a) and (b). The intersections with least and greatest m are stable equilibria, while the intermediate one is a saddle point[2]: in particular there exists a stable separatrix between the saddle point and the leftmost equilibrium. We can now project the points in the (V, m) plane along straight lines of equation $u = V - 36m$, where u is a real parameter. These lines are roughly perpendicular to the separatrix of above, which acts as a boundary for the threshold responses: trajectories nearby tend to the leftmost equilibrium, which can be considered a stable excited state, and information about how the trajectories get closer to the separatrix is not important to us, as we are most interested in how trajectories tend to the excited state. By the projection we can use u as a new co-ordinate, losing the component of the vector field which is orthogonal to the separatrix, and maintaining information about the parallel component.

[2] See [4], pages 874-875

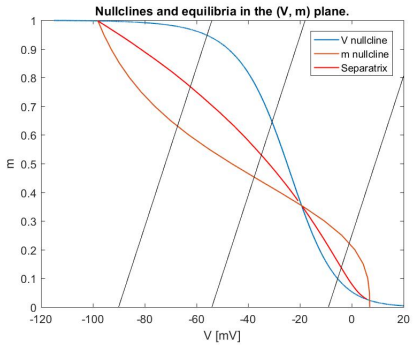

Figure 2.1: The values for the parameters are from [5], pages 509-514-520 (curve J). The black lines in the right figure show the direction of projection.

The (h, n) plane One can see plotting the curves $n(t)$ and $h(t)$ in a same graph (as done in Figure 2.2) that the two curves $-h$ and n have the same shape: this implies that the new coordinate $w = 0.5(n - h)$ is fit to describe the dynamics as well. Notice that $-h$ and n have the same shape if and only if $-h \approx n + k$, for some $k \in \mathbb{R}$ constant. This holds if and only if $\frac{d}{dt}(n + h) \approx 0$. With some computations we can write $\frac{d}{dt}(h + n) = -c(h + n) + e(h - n)$, with

$$c = \frac{\alpha_n + \beta_n - \frac{\alpha_n}{n} - \alpha_h + \beta_h + \frac{\alpha_h}{h}}{2}$$
$$e = \frac{\alpha_n + \beta_n - \frac{\alpha_n}{n} + \alpha_h - \beta_h - \frac{\alpha_h}{h}}{2}$$

It turns out that during an action potential, after an initial short transient, c and e tend to be constant, with $c > 0$, $c \approx -10e$. Changing variables to $y = h + n$, $x = h - n$, we have a system where $\dot{y}$ is largely determined by y itself,and therefore y is attracted (after the transient) by the straight line passing through the origin with slope $\frac{ex}{c}$. Since x given its definition can take values in $[0, 1]$ only, we can expect a variation in $y = n + h$ of no more than $\frac{1}{10}$. We can simulate the system to find minimum and maximum of $\frac{d}{dt}(n + h)$ to get a better estimate. in particular we get that the derivative must be less than or equal to 0.2292 s^{-1} and greater than or equal to -0.0034 s^{-1}. Since the time required for an action potential to take place is of about 25×10^{-3} s, $n + h$ cannot vary more than 0.006, hence it is almost constant.

2.2.2 The (u, w) plane

Now we have the necessary information to compare the reduced (u, w) system with a system described by the equations in (2.2). Figure 2.3 was obtained solving with MATLAB Hodgkin-Huxley equations, and then plotting the quantities

$$\begin{cases} u &= V - 36m \\ w &= 0.5(n - h) \end{cases}$$

We can easily see that trajectories in the reduced plane (u, w) approximately resemble the ones in Figure 2.4. A complete and detailed comparison of the two

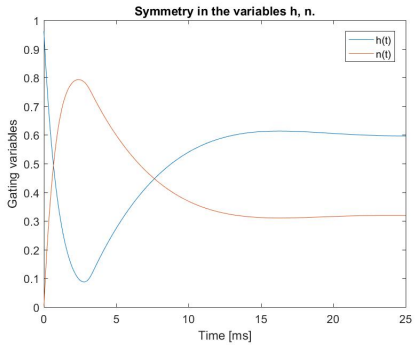

Figure 2.2: Evolution of h, n over time. $V_0 = -60$ mV.

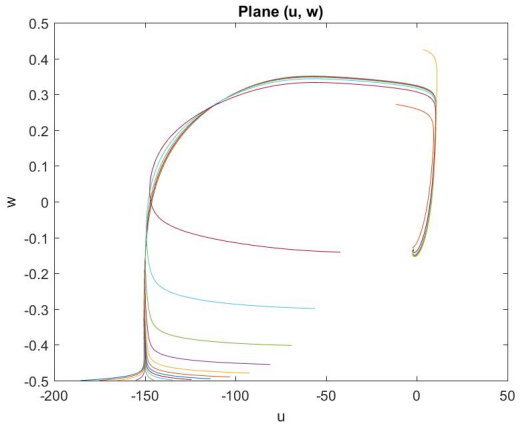

Figure 2.3: Trajectories for various initial voltages.

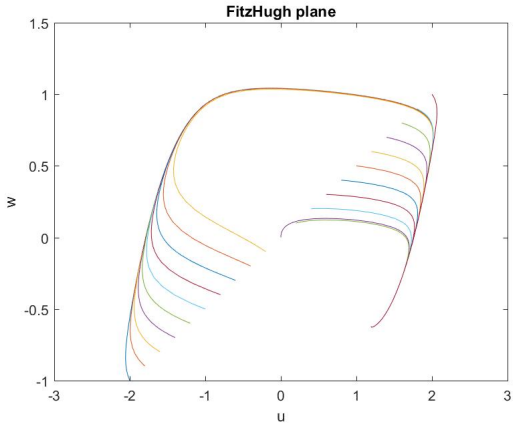

Figure 2.4: Trajectories described by FitzHugh's equations.

models can be found in [2], and it is not the aim of this dissertation. However, in the words of Keener and Sneyd in [6],

"There is considerable value in studying systems of equations that are simpler than the Hodgkin–Huxley equations but that retain many of their qualitative features. This is the motivation for the FitzHugh–Nagumo equations and their variants."

2.3 Analysis of FitzHugh-Nagumo systems

2.3.1 The case $z = 0$

First we want to find the equilibria of the system, and then show their dynamical properties. The two nullclines have equations:

$$\begin{cases} w = -u + \frac{u^3}{3} & u \text{ nullcline} \\ w = \frac{a-u}{b} & w \text{ nullcline} \end{cases}$$

so the equilibrium points need to satisfy the algebraic equation

$$\frac{u^3}{3} + \left(\frac{1}{b} - 1\right) u - \frac{a}{b} = 0 \tag{2.8}$$

We want to prove that this polynomial has only one real root, and that the

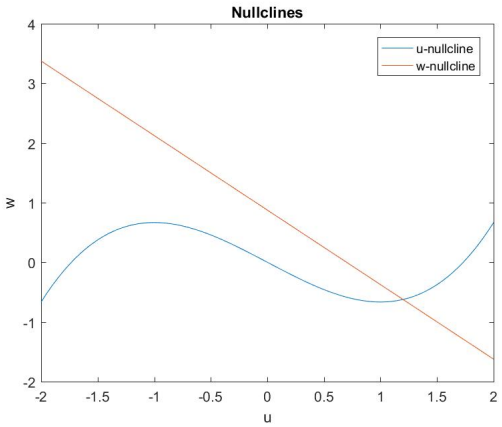

Figure 2.5: Nullclines in FN. $z = 0, a = 0.7, b = 0.8, c = 3$.

corresponding point in the state space is a Lyapunov-stable equilibrium. By the theory of polynomials we know that if the discriminant of a polynomial function of third degree is negative, such a function has only one real zero. In this case the discriminant is

$$\Delta = \frac{-4 + 12b - 27a^2b - 12b^2 + 4b^3}{b^3}$$

As $b > 0$ to prove the thesis we can show that the expression $-4 + 12b - 27a^2b - 12b^2 + 4b^3$ $(*)$ is strictly less then 0. Recall now that $a > 1 - \frac{2b}{3}$: this inequality

implies that $(*)$ is less than the following expression:

$$p(b) = -8b^3 + 24b^2 - 15b - 4$$

If we now show that $p(b) < 0$ for all $b \in]0,1[$ we are done. Observe that $p(0) = -4$, and that the derivative $p'(b)$ is greater than or equal to 0 if and only if $0.3875 \leq b \leq 1.6125$. In particular 0 and 1 are points of local maximum given the constraints of the system, and $p(1) = -3$: thus $p(b) < 0$ in $]0,1[$, and we have only one equilibrium.
Let us now consider the linearised system: the Jacobian matrix of the vector field is

$$J = \begin{pmatrix} c(1-u^2) & c \\ -\frac{1}{c} & -\frac{b}{c} \end{pmatrix}$$

We can infer the sign of the real part of the eigenvalues from the following conditions:

$$\begin{cases} \mathrm{tr}(J) \geq 0 \\ \det(J) \geq 0 \end{cases}$$

By the constraints on the parameters we get that $\det(J) > 0 \Leftrightarrow u^2 > 1 - \frac{1}{b}$ holds for any admissible value of u, so the interesting condition is given by the first inequality. $\mathrm{tr}(J) < 0$ if and only if $|u| > \sqrt{1 - \frac{b}{c^2}}$: in this case the two eigenvalues need to have negative real part. In particular, to prove Lyapunov-stability it suffices to show that if a point (u^*, w^*) is an equilibrium (and in particular u^* satisfies equation 2.8) then the trace of the matrix J at that point is negative. We prove the contrapositive: assume that the trace for some value u is strictly positive, and show that u cannot satisfy equation 2.8. In order to do this, we need to assume the constraints on the parameters a, b, c. Firstly, u cannot be negative or zero, or it cannot satisfy the equation. If $0 < u \leq \sqrt{1 - \frac{b}{c^2}}$ we get the following inequalities:

$$\begin{aligned} \frac{u^3}{3} + \left(\frac{1}{b} - 1\right) - \frac{a}{b} &\leq \left(1 - \frac{b}{c^2}\right)\sqrt{1 - \frac{b}{c^2}} \cdot \frac{1}{3} + \left(\frac{1}{b} - 1\right)\sqrt{1 - \frac{b}{c^2}} - \frac{a}{b} < \\ &< \left(1 - \frac{b}{c^2}\right)\sqrt{1 - \frac{b}{c^2}} \cdot \frac{1}{3} + \left(\frac{1}{b} - 1\right)\sqrt{1 - \frac{b}{c^2}} - \frac{1}{b}\left(1 - \frac{2b}{3}\right) = \\ &= \sqrt{1 - \frac{b}{c^2}}\left(-\frac{b}{3c^2} + \frac{1}{b} - \frac{2}{3}\right) - \frac{1}{b} + \frac{2}{3} < \\ &< \sqrt{1 - \frac{b}{c^2}}\left(-\frac{\not{b}}{3\not{b}} + \frac{1}{b} - \frac{2}{3}\right) - \frac{1}{b} + \frac{2}{3} < \\ &< \sqrt{1 - \frac{b}{c^2}} - 1 - \sqrt{1 - \frac{b}{c^2}} + \frac{2}{3} < 0 \end{aligned}$$

and the point cannot be an equilibrium. Therefore the only equilibrium needs to be a sink.
We shall now prove that trajectories from any starting point $x = (u, w)$ are defined for any $t \in \mathbb{R}$. We shall need the following Lemma, which we are not going to prove:

Lemma 2.3.1. *Let x be a point in the state plane. Suppose that the forward orbit of x lies in a compact subset of the state plane. Then $\phi_t(x)$ is defined for*

any $t \geq 0$, where ϕ is the flow associated to the system of ODEs describing the system.

Assume, for contradiction, that $J = [0, T[$ is a maximal interval on which a solution is defined, for some $T \in \mathbb{R}^{>0}$. By previous lemma it holds that $\limsup_{t \nearrow T} \|\phi_t(x)\| = \infty$, or otherwise the flow would be confined in a compact set of $\mathbb{R}^2$, and $T = \infty$. It must hold therefore that $\limsup_{t \nearrow T} \frac{d}{dt}\|\phi_t(x)\|^2 \geq 0$. However the set where $\frac{d}{dt}\|\phi_t(x)\|^2 \geq 0$ can be determined the following way:

$$\begin{aligned} \frac{d}{dt}\|\phi_t(x)\|^2 = 2\phi_t(x) \cdot \dot{\phi}_t(x) = 2 \begin{pmatrix} u \\ w \end{pmatrix} \cdot \begin{pmatrix} \dot{u} \\ \dot{w} \end{pmatrix} \geq 0 \\ \Leftrightarrow c\left(uw + u^2 - \frac{u^4}{3}\right) - \frac{uw - aw + bw^2}{c} \geq 0 \end{aligned}$$

and the set defined by this last inequality is compact: we have a plot of a particular case obtained using Mathematica in Figure 2.6. It is closed as it is the preimage of a closed set under a continuous function, and we can see that it is bounded passing to polar coordinates on the (u, w) plane: defining

$$\begin{cases} u = r\cos\theta \\ w = r\sin\theta \end{cases}$$

the set can be written as $\{\Phi(r, \theta) \geq 0\}$, where $\Phi : \mathbb{R}^2 \to \mathbb{R}$,

$$\Phi(r,\theta) = c\left(r^2 \sin\theta\cos\theta + r^2\cos^2\theta - \frac{r^4\cos^4\theta}{3}\right) - \sin\theta\frac{r^2\cos\theta - ar + br^2\sin\theta}{c}$$

One can easily see that if $\theta \notin \left\{\pm\frac{\pi}{2}\right\}$ then the dominant term for large values of r

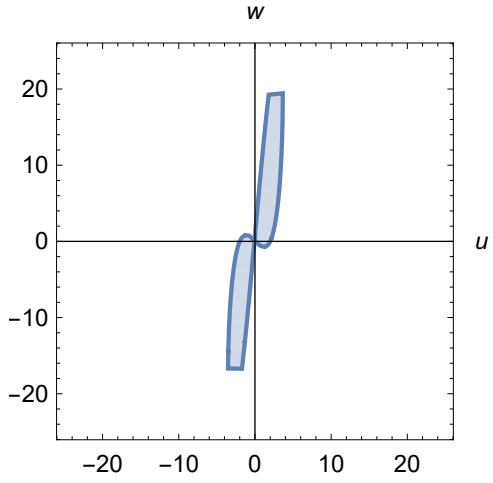

Figure 2.6: The region where $\frac{d}{dt}\|\phi_t(x)\|^2 \geq 0$, for the values $a = 0.7$, $b = 0.8$, $c = 3$.

is $-c\frac{r^4\cos^4\theta}{3} \xrightarrow{r\to\infty} -\infty < 0$. If $\theta = \frac{\pi}{2}$, then $\Phi(r, \frac{\pi}{2}) = \frac{ar}{c} - \frac{br^2}{c} \xrightarrow{r\to\infty} -\infty < 0$, and if $\theta = -\frac{\pi}{2}$ we again have that $\Phi(r, -\frac{\pi}{2}) = -\frac{ar}{c} - \frac{br^2}{c} \xrightarrow{r\to\infty} -\infty < 0$. In

each of these cases by continuity we infer that $\Phi(r,\theta) < 0$ for large enough values of r: therefore $\{\Phi(r,\theta) \geq 0\}$, the set we are interested in, is bounded, and therefore compact. But this leads to contradiction, as we assumed that $\limsup_{t \nearrow T} \|\phi_t(x)\| = \infty$.
The proof can be repeated for negative times: therefore trajectories are defined for any real time t. We now show that trajectories are always contained in a bounded set. We already know that they are defined for any $t \in \mathbb{R}$, so if for a particular initial value x (which we can assume to be 0, up to translation of the system) the orbit is unbounded, there is a sequence of positive times $t_k \to \infty$ such that $\|\phi_{t_k}(0)\| \to \infty$. Consider again the bounded set where $\frac{d}{dt}\|\phi_t(x)\| \geq 0$, let $R > 0$ be such that $B(0,R]$ (closed ball of radius R and centre 0) contains this set. Let t_j be an element of the sequence of times such that $\|\phi_{t_j}(0)\| > R$, and $t^* < t_j$ the last positive time before t_j such that $\|\phi_{t^*}(0)\| = R$. By the Fundamental Theorem of Calculus we have that:

$$R < \|\phi_{t_j}(0)\| = \int_0^{t_j} \frac{d}{dt}\|\phi_t(0)\| d\, t = \int_0^{t^*} \frac{d}{dt}\|\phi_t(0)\| d\, t + \int_{t^*}^{t_j} \frac{d}{dt}\|\phi_t(0)\| d\, t < R$$

as $\frac{d}{dt}\|\phi_t(0)\| < 0$ for any $]t^*, t_j]$. This is a contradiction, and the orbits are therefore forced to be bounded.
We now consider horizontal displacements from the equilibrium P: P in our model has the meaning of resting state of the neuron, studying what happens to orbits after a horizontal displacement is meaningful as it corresponds to a qualitative study of how the neuron reacts to an instantaneous change in the voltage. Initial vertical displacements instead correspond to variations in the gate variables h, n only, so they are not as easily physiologically justified. A key observation here is that the absence of an upper bound for c forces the variables u, w to change at different rates: setting $\varepsilon = c^{-1}$ we can rewrite the system as follows:

$$\begin{cases} \varepsilon \dot{u} = w + u - \frac{u^3}{3} \\ \dot{w} = -\varepsilon(u - a + bw) \end{cases}$$

and, since ε can be much smaller than 1, u is the fast variable and w the slow one. In particular, outside the nullclines, we have $|\frac{\dot{u}}{\dot{w}}| \approx \varepsilon^{-2} = c^2 \ggg 0$. Thanks to this discussion we can again consider w constant and describe the behaviour of the system as it was done for HH (see section 2.2.1).
Consider a constant w: the straight line $\{(u,w) | u \in \mathbb{R}\}$ is then a phase line for the fast subsystem of the variable u. For any constant w the $u-$dynamics can be described studying the position of the phase line with respect to the $u-$nullcline. Consider r, a straight horizontal line through the equilibrium P. Above we proved that if u_P is the $u-$coordinate of P, the condition

$$0 < u_P \leq \sqrt{1 - \frac{b}{c^2}}$$

leads to contradiction for any b, c, so necessarily $u_P > 1$, and r has three intersections with the $u-$nullcline. Studying the equations it is immediate to see that $\dot{u}(u,w) \geq 0$ if and only if $w \geq \frac{u^3}{3} - u$, and thus the three intersections of the $u-$nullcline are, from left to right, an attractive equilibrium (for u only, so we call it **excited point**), a repelling equilibrium (again, for u only), and a stable equilibrium (for the whole system). Given this characterisation of the intersections, we start by noticing that an initial point to the right of P or between P

and the unstable intersection rapidly goes back to P. If the initial point lies instead at the left of the repelling equilibrium for the fast subsystem (second intersection), the trajectory moves quickly towards the attractive equilibrium to the left. When the orbit reaches the excited point, the $w-$dynamics dominate, and since $\dot{w}(u,w) \geq 0$ if and only if $w \leq \frac{a-u}{b}$, w increases slowly: the phase line moves upwards, and the trajectory tends to stay at the excited point, i. e. follows (approximately) the $u-$nullcline. At a certain moment the the phase line ceases to have three different intersections with the $u-$nullcline: the two leftmost ones collapse into a saddle point, and the orbit then moves rightwards, getting farther from the $u-$nullcline, so that the $w-$dynamics get back to being negligible. The movement becomes horizontal once again, and tends to the only attractive equilibrium which is left on the phase line. When this is reached, again the w-dynamics dominate, and this time the trajectory moves downwards, until P is reached.
For initial displacements to the left of the leftmost intersection the description is similar, as the trajectories tend to the excited point and then behave as shown above.
Given this behaviour, one might argue that the intersection which gives rise to

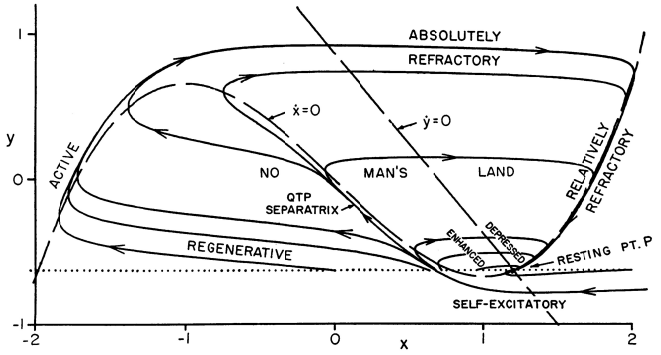

Figure 2.7: Possible trajectories for horizontal displacements from the equilibrium, [2], page 448. $x = u$, $y = w$.

the unstable equilibrium for the fast subsystem acts like a **threshold**: mathematically, this means that, if $\vec{\gamma} = \pm\gamma\hat{u}$, there exists some time time $\hat{t}$ such that $\phi_{\hat{t}}(P + \vec{\gamma})$ is discontinuous as a function of $\vec{\gamma}$. In neuroscience, this behaviour is said to be **all-or-none**. As FitzHugh remarks in [2], page 452, this is not the case for his model: he argues that if initial point lay on the unstable equilibrium and the computer calculations were errorless we would not have any discontinuity, as the trajectory would follow the u-nullcline upwards and into the region which in Figure 2.7 is labelled as *No Man's Land* (consistently with the analysis of above), hence we would have all the intermediate behaviours between *all* (trajectories reaching the excited point) and *none* (trajectories going immediately back to P). FitzHugh calls this a **Quasi-Threshold Phenomenon**, as defined in [3], page 265: the flow as a function of $\vec{\gamma}$ simply fails to be Lipschitz (or has a large

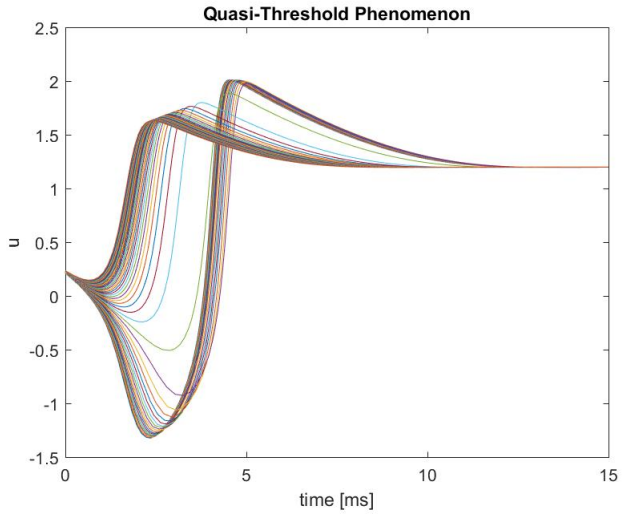

Figure 2.8: Plot of u over time for evenly spaced points with same $w-$coordinate.

Lipschitz constant), but remains continuous, as we can see in Figure 2.8. We shall write about this in the next paragraph.
Extension of the observations from above to the case of non-horizontal displacements is immediate: given the initial point, if it does not lie on the $u-$nullcline, we can repeat the study of the fast subsystem's dynamics. If it lies on that nullcline the $w-$dynamics dominate, and the point follows the $u-$nullcline if the initial point is a stable equilibrium for the fast subsystem, or rapidly goes far from the curve if it is unstable instead.
To conclude, it remains to explain the meaning of the labels in Figure 2.7: the *enhanced* region is a set of points for which the necessary displacement to tend to the excited point is less than the one required for P (indeed, they lie between P and the middle intersection). The *regenerative* region is the one where the trajectories tend to the excited points without needing any further stimulus. As described above, the *active* phase takes place when the orbit follows closely the $u-$nullcline. The *absolutely refractory* region contains the points above the left local maximum of the $u-$nullcline: the phase line does not contain any excited point, so going back to the *active* phase is clearly impossible with a horizontal displacement. The *relatively refractory* and the *depressed* regions contain the points for which getting back to the active state is possible, but the necessary displacement is greater than the one needed to activate P.

FitzHugh's canards

In this paragraph we want to apply the theory developed in Chapter 3 of [8]. To proceed, consider a rescaling of time $t = \varepsilon\tau$, which applied to the system gives the equivalent description:

$$\begin{cases} \frac{d}{d\tau}u = w - \frac{u^3}{3} + u \\ \frac{d}{d\tau}w = -\varepsilon^2[u - a + bw] \end{cases}$$

and by arbitrariness of the choice of ε replace ε^2 with ε (notice that now the condition on b becomes $b < \min\{1, \varepsilon^{-1}\}$), and for simplicity relabel τ with t. The ODE we obtain this way is the following:

$$\begin{cases} \dot{u} = w - \frac{u^3}{3} + u \\ \dot{w} = -\varepsilon[u - a + bw] \end{cases} \tag{2.9}$$

We can now give definitions which will be useful in the following discussion.

Definition 2.3.1 (Fast-slow systems)**.** An (m, n)-fast-slow system is an ODE in one of the two forms:

$$\begin{cases} \varepsilon\dot{x} = f(x, y, \varepsilon) \\ \dot{y} = g(x, y, \varepsilon) \end{cases} \tag{2.10}$$

$$\begin{cases} \dot{x} = f(x, y, \varepsilon) \\ \dot{y} = \varepsilon g(x, y, \varepsilon) \end{cases} \tag{2.11}$$

We say that the first ODE is written in the slow time-scale, and that the second one is written in the fast time-scale. Notice that this convention makes sense as one can pass from one expression to the other via a reparametrisation of time.

Comparing (2.9) and (2.11) one immediately sees that:

$$f(u, w, \varepsilon) = w - \frac{u^3}{3} + u \tag{2.12}$$

$$g(u, w, \varepsilon) = -(u - a + bw) \tag{2.13}$$

Definition 2.3.2 (Critical set)**.** Consider the system in (2.11), and define its critical set as follows:

$$C_0 = \{(x, y) \in \mathbb{R}^{m+n} | f(x, y, 0) = 0\}$$

If C_0 is a submanifold of $\mathbb{R}^{m+n}$, C_0 will be called "critical manifold".

In other words, the critical set is the subset of the phase space where the dynamics are completely determined by the system:

$$\begin{cases} 0 = f(x, y, 0) \\ \dot{y} = g(x, y, 0) \end{cases} \tag{2.14}$$

whose flow is called "slow flow". Applying definition (2.3.2) to system (2.9) we see that C_0 in our case is nothing but the $u-$nullcline.

Definition 2.3.3 (Normally hyperbolic set)**.** A set $S \subset C_0$ is said to be normally hyperbolic if all the eigenvalues of $\nabla_x f(p, 0)$ have nonzero real part for all $p \in S$. $\nabla_x f$ here is the Jacobian matrix of f with respect to the fast variables. If all the eigenvalues have positive real part, S is sad to be repelling, if they have all negative real part S is attractive. If S is normally hyperbolic but neither attractive nor repelling S is said to be of saddle type.

We shall often require compactness of S.

Proposition 2.3.2. *$S \subseteq C_0$ is normally hyperbolic if and only if $\forall p = (x^*, y^*) \in S$, x^* is a hyperbolic equilibrium point for the system $\dot{x} = f(x, y^*, 0)$.*

Proof. Let $p \in S$. Then $f(p,0) = 0$, so x^* is an equilibrium for $\dot{x} = f(x, y^*, 0)$. The condition on the Jacobian matrix gives the hyperbolicity. For the other implication, let x^* be a hyperbolic equilibrium for $\dot{x} = f(x, y^*, 0)$: then $f(p,0) = 0$, so $p \in S$, and again the condition on the Jacobian is satisfied by hyperbolicity. □

Definition 2.3.4 (Hausdorff distance)**.** Let $\mathcal{K}(\mathbb{R}^n)$ be the set of the compact subsets of $\mathbb{R}^n$ with the standard topology, $\|\cdot\|$ be the Euclidean norm. Define the Hausdorff distance on $\mathcal{K}(\mathbb{R}^n)$: for every $V, W \in \mathcal{K}(\mathbb{R}^n)$

$$d_H(V,W) = \max\left\{\sup_{v\in V}\inf_{w\in W}\|v-w\|, \sup_{w\in W}\inf_{v\in V}\|v-w\|\right\}$$

Remark. The Hausdorff distance measures "how much two sets overlap"and "are similar". The compactness is required for d_H to be well defined (i. e. not infinity) and a metric (immediate to see that otherwise the distance between a set and its closure is 0).

In the statement of the following theorem, the slow manifold is defined. We will need this notion to proceed with our study of the canards.

Theorem 2.3.3 (Fenichel 1979)**.** *Let S_0 be a compact normally hyperbolic submanifold (possibly with boundary) of C_0, $f, g \in \mathcal{C}^r$. For any $\varepsilon > 0$ small enough the following hold:*

i) There exists a manifold S_ε diffeomorphic to S_0. S_ε is locally invariant: for any $p \in S_\varepsilon$ there exists an interval $I =]t_1, t_2[$ so that $\phi_t(p) \in S_\varepsilon$ for all $t \in I$.

ii) $d_H(S, S_\varepsilon) = \mathcal{O}(\varepsilon)$ as $\varepsilon \to 0$.

iii) The flow on S_ε converges to the slow flow as $\varepsilon \to 0$.

iv) S_ε is $\mathcal{C}^r$-smooth.

v) S_ε is still normally hyperbolic, and the stability characteristics are the same as for S.

vi) S_ε is usually not unique.

Proof. Omitted, see [1]. □

Despite point *iv)* we shall say "the slow manifold"to indicate any of the possible slow manifolds.
Reduce now to the case of system (2.9). As above said C_0 is the $u-$nullcline, and since $\nabla_u f(u,w,0) = 1 - u^2$, we infer that all points with $u \neq \pm 1$ are hyperbolic, therefore any compact submanifold in contained in the middle branch is normally hyperbolic and repelling, and any compact submanifold of the left or right branch of C_0 is normally hyperbolic and attracting.

Definition 2.3.5 (Canard)**.** A solution is called a canard if it stays at a distance $\mathcal{O}(\varepsilon)$ from the repelling branch of a slow manifold for a time $\mathcal{O}(1)$ in the slow time-scale $\tau = t\varepsilon$.

Now apply Theorem 2.3.3 to 2.9: consider a compact normally hyperbolic submanifold of the middle branch of C_0, let it be S, and assume it disjoint from the $w-$nullcline. By these hypotheses, S has a boundary given by two points P_0, P_1, both in the middle branch of the nullcline. We want to show that for ε small enough no slow manifold can be fully contained in the area of plane above the u-nullcline, and to do so we use points $i)$ and $ii)$ of Fenichel's Theorem. First observation: by point $i)$ any slow manifold is a compact curve which is locally invariant, and this means that trajectories can get in and out this curve only through its boundary. This condition forces the slow curve "to have the same shape as the dynamics". Let $\gamma(t) = (u(t), w(t))$ be a generic solution of the system, for any initial value: its temporal derivative is $\dot{\gamma} = (\dot{u}(u,w), \dot{w}(u,w))$, and in particular in the region above S, between the $u-$nullcline and the $w-$nullcline, both components of the derivative are positive, in the region below S one has $\dot{u} < 0$, $\dot{w} > 0$ instead. We want to show that for ε small enough the slow manifolds need to "follow"S, generating contradiction if the slow curve is fully contained in the region above S, and to do so we use point $ii)$. Let Γ be the $w-$nullcline (the straight line) and

$$d(A,B) = \inf\{\|a-b\| \,|a \in A, b \in B\}$$

for two sets A and B. Consider now

$$\lambda = \min\{\|(P_0 - P_1)_u\|, \|(P_0 - P_1)_w\|, d(S,\Gamma)\}$$

Since S is compact and Γ is closed we have that $d(S,\Gamma) > 0$. By point $ii)$ there exists some positive constant $k \in \mathbb{R}$ so that if $\varepsilon \to 0$ then $d_H(S, S_\varepsilon) < k\varepsilon$: choose then an ε that gives us $k\varepsilon < \frac{\lambda}{3}$. By definition of Hausdorff distance there exist points Q_0 and Q_1 so that $\|P_0 - Q_0\| < k\varepsilon$, $\|P_1 - Q_1\| < k\varepsilon$, and assume by contradiction that both the points lie above C_0. By local invariance they are connected by the flow, and therefore by definition of Hausdorff distance the branch of curve in between is fully contained in the region of plane between C_0 and Γ: for contradiction, assume there exists some $\bar{Q}$ beyond Γ. By continuity of the flow there needs to be some $\{Q'\} \subset S_\varepsilon \cap \Gamma$, and this is a contradiction: by definition of Hausdorff distance $d(Q', S) < d(S,\Gamma)$ (where the point-set distance is the infimum of the distances of the points of the set from the specified point) because $Q' \in S_\varepsilon$, and $d(Q', S) \geq d(S,\Gamma)$ because $Q' \in \Gamma$. Since we did not specify the relative positions of P_0 and P_1 we can now assume that there exists some $t > 0$ such that $\phi_t(Q_0) = Q_1$. Since $\phi_t(Q_0) = Q_1$ we need to have $Q_{0,u} < Q_{1,u}$, $Q_{0,w} < Q_{1,w}$ by the Fundamental Theorem of Calculus (the curve is fully contained in the region where both temporal derivatives are positive). We now have two possible alternatives for the relative positions of P_0 and P_1, both leading to contradiction: $P_{0,u} < P_{1,u}$ and $P_{0,w} > P_{1,w}$, or $P_{0,u} > P_{1,u}$ and $P_{0,w} < P_{1,w}$. Let us consider the first option: by $\|P_0 - Q_0\| < \frac{\lambda}{3}$ we have that $Q_{0,w} \geq P_{0,w} - \frac{\lambda}{3}$ and similarly $Q_{1,w} \leq P_{1,w} + \frac{\lambda}{3}$. From these inequalities we get:

$$Q_{0,w} - Q_{1,w} \geq P_{0,w} - \frac{\lambda}{3} - P_{1,w} - \frac{\lambda}{3} \geq \lambda - 2\frac{\lambda}{3} = \frac{\lambda}{3} > 0 \quad \Rightarrow Q_{0,w} > Q_{1,w}$$

which is a contradiction. In the second case we can proceed in a similar way to get to an analogous contradiction, so the slow curve cannot be fully contained in the region above C_0 for an ε small enough, and the value of ε depends on the

chosen submanifold.
The given argument is enough to prove the existence of canards: choose a compact normally hyperbolic submanifold of C_0 disjoint from Γ, and again call it S, and fix the small ε used in the proof above. The associated slow manifold S_ε then either is contained in the region below C_0 or crosses the $u-$nullcline. If S_ε crosses C_0 it is then forced to go right by local invariance, and it cannot cross C_0 again. Let w_0 be the minimum $w-$coordinate of all the points in S_ε in the region below C_0, and w_1 the maximum. By Fundamental Theorem of Calculus we see that the projection $S_\varepsilon \to \mathbb{R}$, $(u, w) \mapsto w$ is injective, and hence we can compute the necessary time to go through the curve from w_0 to w_1 with the following integral:

$$T = \int_{w_0, S_\varepsilon}^{w_1} \frac{d\, w}{|\dot{w}(u(w), w)|}$$

Write the system in the slow time-scale, and observe that by equation (2.9) we have that $\frac{1}{|\dot{w}|}$ is continuous in a neighbourhood of S_ε. Applying Weierstrass Theorem on a compact contained in such a neighbourhood we have:

$$M(\varepsilon)(w_1 - w_0) \geq T = \int_{w_0, S_\varepsilon}^{w_1} \frac{d\, w}{|u(w) - a + bw|} \geq m(\varepsilon)(w_1 - w_0)$$

where $M(\varepsilon)$ and $m(\varepsilon)$ are respectively global maximum and minimum of $\frac{1}{|\dot{w}|}$ in the compact neighbourhood. If now M and m are respectively maximum and minimum of $|\dot{w}|^{-1}$ on S, since $d_H(S_\varepsilon, S) \xrightarrow{\varepsilon \to 0} 0$ we have $M(\varepsilon) \xrightarrow{\varepsilon \to 0} M$, $m(\varepsilon) \xrightarrow{\varepsilon \to 0} m$ by continuity, and this is enough to prove that $T = \mathcal{O}(1)$. Trajectories following the slow manifolds of the repelling branch of C_0 are therefore canards. By the geometrical features we proved above we infer that they cannot lie completely to the right of S, and this confirms FitzHugh's observations of trajectories following the repelling branch of C_0 and then bend suddenly to the left.

2.3.2 The perturbed system

We now remove the hypothesis $z = 0$. To start, we need to compute again number and dynamical features of the equilibria. By hypothesis z is independent to u, so the study of the number of the real solutions of the algebraic equation

$$\frac{u^3}{3} + \left(\frac{1}{b} - 1\right) u - \frac{a}{b} - z = 0$$

which are the $u-$coordinates of the equilibria, reduces to the study of the injectivity and surjectivity of the function $h(u) = \frac{u^3}{3} + \left(\frac{1}{b} - 1\right) u$. We can immediately see that $h'(u) > 0$ for all u, therefore the function in injective. h is a cubic polynomial, so $\lim_{u \to \pm\infty} h(u) = \pm\infty$, and by continuity (intermediate value theorem) h is surjective. By bijectivity of h the algebraic equation, for any fixed z, has only one real solution, and the system has still precisely one equilibrium. We want to repeat the procedure we followed when studying the dynamics near the equilibrium in the resting system: the Jacobian matrix is still the same, hence we have the same conditions on the $u-$coordinates, but the algebraic condition for the equilibrium is different. Consider again the conditions:

$$\begin{cases} \mathrm{tr}(J) \geq 0 \\ \det(A) \geq 0 \end{cases}$$

The second one holds trivially. Again, $\mathrm{tr}(J) \geq 0 \Leftrightarrow |u| \leq \sqrt{1 - \frac{b}{c^2}}$ and if $z \geq 0$ we can use again the estimates used in the case $z = 0$ to conclude the stability of the equilibrium. For $z < 0$ those estimates fail. Geometrically, a change in the parameter z moves up and down the $u-$nullcline, which can be divided into three regions, according to the sign of its $u-$derivative. As this nullcline is described by the equation $w = \frac{u^3}{3} - u - z$, its u-derivative is positive for u outside the interval $[-1, 1]$, and less than or equal to 0 inside. The upwards or downwards shift of the nullcline also shifts the point of equilibrium from a branch of the $u-$nullcline to another, and this change has consequences on the stability of the equilibrium: observe that in particular if the $u-$derivative of the u-nullcline is positive, then the trace of the Jacobian needs to be negative (it suffices to compare the inequalities) and the equilibrium is stable. Now, notice that there exists at least one value of z that causes the equilibrium to be unstable: set $z = -\frac{a}{b}$ and observe that given the geometrical interpretation it is obvious that the intersection of the nullclines has now $u-$coordinate 0. The equilibrium is in this case a source as trace and determinant are both strictly positive. The operations which are used in finding the root of the third degree polynomial are continuous, so the function $z \mapsto u_z$, where u_z is the $u-$coordinate of the equilibrium, is continuous; by the condition on $\mathrm{tr}(J)$ we infer that if z takes value in a neighbourhood of $-\frac{a}{b}$ then the equilibrium is unstable.
We can apply now Poincaré-Bendixson Theorem, but before the statement we need to introduce the proper terminology and notation.

Definition 2.3.6 (α, $\omega-$limits)**.** Given a system described by the differential equation $\dot{x} = f(x)$, $f : X \to X$ and a point $x_0 \in X$, we define the ω-limits of x_0 as the points $y \in X$ such that there exists a monotone increasing sequence $(t_k) \subset \mathbb{R}$ satisfying $\phi_{t_k}(x_0) \xrightarrow{k\to\infty} y$. Similarly we can define the $\alpha-$limits for x_0: they are the points $y \in X$ such that there exists a monotone decreasing sequence satisfying $\phi_{t_k} \xrightarrow{k\to-\infty} y$.

Definition 2.3.7 (α, ω-limit sets)**.** Let us consider the system $\dot{x} = f(x)$, $f : X \to X$, $x_0 \in X$. We can define the ω-limit set of x_0 as follows:

$$\omega(x) = \{\, y \in X \mid y \text{ is an } \omega - \text{limit of } x_0 \,\}$$

and similarly the α-limit set:

$$\alpha(x) = \{\, y \in X \mid y \text{ is an } \alpha - \text{limit of } x_0 \,\}$$

We can now state the theorem.

Theorem 2.3.4 (Poincaré-Bendixson)**.** *Let us consider the system $\dot{x} = f(x)$, $X = \mathbb{R}^2$, $f \in \mathcal{C}^1(X)$ with associated flow ϕ. If $\phi_t(x) \subset K \subset X \, \forall t \geq 0$, K compact, then either one of the following holds:*

(a) $\omega(x)$ contains a fixed point;

(b) $\omega(x)$ contains a periodic orbit.

A periodic orbit which is an ω-limit set for some point in the state plane is said to be a **limit cycle**. If we prove that each trajectory is bounded, by Poincaré-Bendixson Theorem, using the fact that the only equilibrium is a source,

we infer the existence of a limit cycle. We can use again the same estimate we made above (after Lemma 2.3.1): repeating the calculations we notice that the presence of z adds a term of first degree in r, which is therefore negligible and the same conclusions hold. This is enough to infer the existence of this curve, and the fact that any trajectory with any starting point (apart from the equilibrium) tends to a limit cycle. If we now plot the projection into the $u-$axis of a trajectory over time for this system we get a train of infinite spikes, and this train cannot be finite given the existence of a limit cycle. In

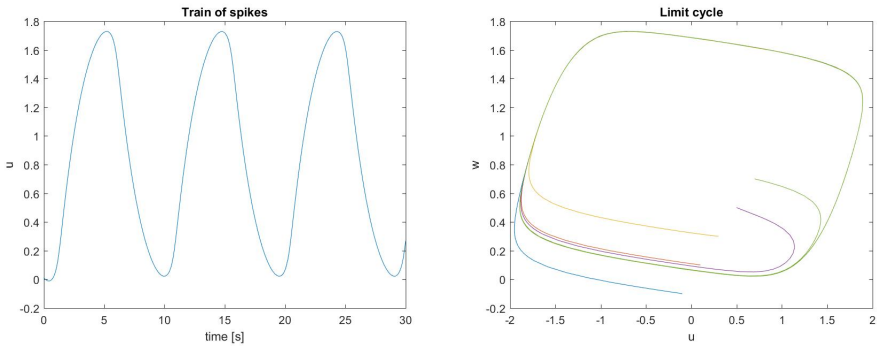

(a) (b)

Figure 2.9: $a = 0.7, b = 0.8, c = 3, z = -\frac{a}{b}$, and the unstable equilibrium is at $(0, \frac{7}{8})$.

Figure 2.9 we can see both the train of spikes and the limit cycle. We want now to perform a study similar to the one lead in the previous section about the trajectories of the system. In the interpretation we have given to the variable u, as already mentioned, a horizontal displacement corresponds to a shock given by an instantaneous change of z: according to the geometric role played by the variable, a decrease (resp. increase) moves upwards (resp. downwards) the $u-$nullcline in an instant, and the point moves leftwards (resp. rightwards), then the phase plane goes back to the resting state and we have the displacement. Let us consider the interesting case where the equilibrium of the system is unstable, and we have a limit cycle (the study in the case of a stable equilibrium is not substantially different from what has already been done). Let P be, once again, the equilibrium: necessarily it lies on the middle branch of the u-nullcline, and the phase line has three intersections with the $u-$nullcline. The leftmost and the rightmost ones are two excited points (partial equilibria), the middle one is P, the source of the whole system. If our starting point is to the right of P it is attracted towards the right excited point, and then the w-dynamics force the trajectory to go downwards, until the two rightmost intersections of the phase line with the $u-$nullcline collapse. At this point, the trajectory needs to head towards the intersection on the left branch, which is attractive. Once it is reached, the $w-$dynamics force it to go upwards following the $u-$nullcline, until the two left intersections collapse, when the $u-$dynamics become predominant again and tend to the excited point on the right. Now the system will follow once again the right branch of the $u-$nullcline, and therefore the limit cycle is generated.

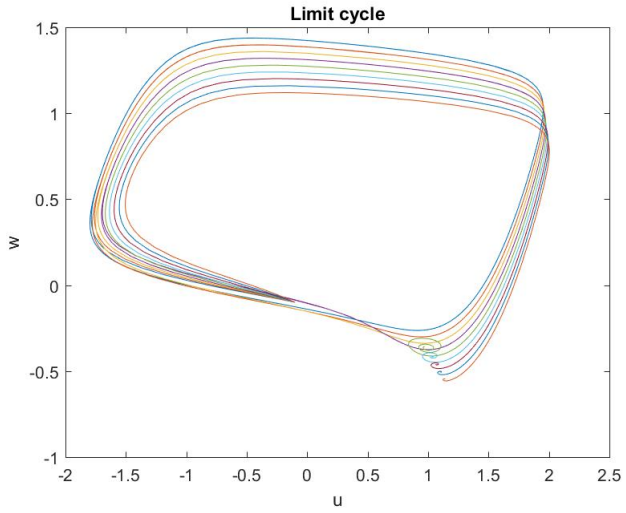

Figure 2.10: Trajectories for the same initial value but different values of z.

The case of displacements to the left is very similar, and the conclusions (trajectories following the nullcline and travelling horizontally from one branch to another, generating the limit cycle) identical.
Let us notice an apparent contradiction: for P to be unstable it is necessary that u_P lay in an interval strictly contained in $[-1, 1]$, so it needs to lie in the middle branch of the $u-$nullcline, but this condition is not a characterisation of the instability. In our discussion although P is always an unstable equilibrium for the fast subsystem, and $u_P \in [-1, 1]$ is a characterisation of the instability in this case. We now need to see that the dynamics of the fast subsystem are representative of the dynamics of the whole system if and only if ε in the definition is sufficiently small, and in particular for $\varepsilon = 0$ we are considering the fast subsystem only, so tautologically its dynamics are all the dynamics. The requirement on ε in our case is strictly connected to the region allowed for an unstable equilibrium: recall that for the equilibrium P to be unstable we need $|u_P| < \sqrt{1 - b\varepsilon^2}$, so asymptotically the fact that P lies in the middle branch of the nullcline becomes a characterisation of the instability, and we solve the apparent contradiction. To appreciate how the analysis fails in case of a small c (large ε), look at Figure 2.11.
A stimulus lasting in time does not require a different description: as FitzHugh explains in [2] at page 454, the only difference is the fact for times long enough that the consequent movement from the equilibrium might have a vertical component, and the argument is the same as above. As before, assume the starting point at the equilibrium P, and firstly assume P to be stable on the right branch of the $u-$nullcline. If the sustained stimulus is positive, the $u-$nullcline moves downwards, and the new equilibrium is still attractive, so the point (provided that the stimulus is kept long enough) reaches it. When the current (z) goes back to its previous value, on the phase line only the left excited point is left, so the trajectory reaches it and then completes the impulse, going back to P: we speak of **cathodal excitation**. If P lies on the left branch instead, and apply the positive stimulus, the behaviour is symmetric and the trajectory goes

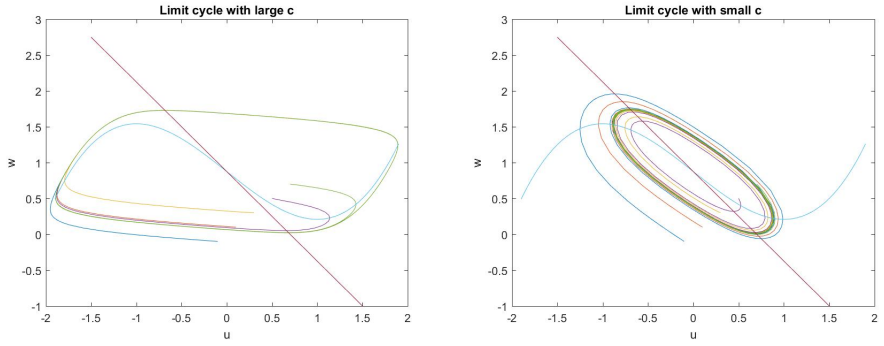

(a) $c = 3$ (b) $c = 1$

Figure 2.11: $a = 0.7, b = 0.8, z = -\frac{7}{8}$. The nullclines are present in both plots, and in b) it is evident that trajectories do not follow the $u-$nullcline at all.

rightwards, and if it goes far enough beyond the threshold, once recovered the resting value of z, we have an impulse. If P lies on the right branch again but the impulse is negative, the $u-$nullcline moves upwards, and similarly the point can travel beyond the threshold to generate a whole impulse. If P lies on the left branch and we apply a negative stimulus the behaviour is symmetrical to the first case: the new equilibrium is reached, then the point travels towards the right branch, the impulse follows. Now let P be unstable on the middle branch. For small variations of z we still have an attractive limit cycle, and the trajectory follows this. Once the resting value of z is established again, the trajectory tends to the original limit cycle.

2.4 Generalisations of FitzHugh-Nagumo

The form for the FN equations we adopted through our discussion is only one of the many available alternatives: in [6] for example **FitzHugh-Nagumo** systems are defined as obeying the following ODE:

$$\begin{cases} \varepsilon \dot{v} = f(v, w) \\ \dot{w} = g(v, w) \end{cases}$$

and the only requirement is on f: it needs to have a *cubic shape*, i.e. "for a finite range of values of w there are three solutions $v = v(w)$ of the equation $f(v, w) = 0$. These we denote by $v = V_-(w)$, $v = V_0(w)$, and $v = V_+(w)$, and, where comparison is possible (since these functions need not all exist for the same range of w), $V_-(w) \leq V_0(w) \leq V_+(w)$". Always in [6], at least three adaptations for the equations are mentioned, and in these the function describing the temporal derivative of the fast variable is piecewise continuous: among these we can find the MacKean model, which given its simplicity allows for explicit solutions, and the Pushchino model, used to describe the ventricular action potential. Nagumo instead, in [11], added a term of dissipation to FitzHugh's equations to describe the propagation of the signal along the axon, obtaining

the PDE which is sometimes called itself *FitzHugh-Nagumo* equation:

$$\begin{cases} h\frac{\partial^2 u}{\partial s^2} = c^{-1}\frac{\partial u}{\partial t} - w - \left(u - \frac{u^3}{3}\right) \\ c\frac{\partial w}{\partial t} + bw = a - u \end{cases}$$

where s denotes the distance along the axon and h is a constant derived from an electronic simulation of FitzHugh's equation, proposed in the same paper. By these contributes Nagumo attached his name to FitzHugh's model.

Chapter 3

The Morris-Lecar Model

In this chapter we are going to introduce and analyse the Morris-Lecar model, first proposed in [10]. Previous studies performed on the barnacle giant muscle fibre had shown that it incorporates a simple system of two conductances, and the ions involved were Ca^{++} and K^+, but in opposition to the case studied by Hodgkin and Huxley in [5] neither conductance shows fast inactivation. Although in physiological conditions this does not allow for a wide range of allowed behaviours for the voltage, in experimental conditions (after injection of EGTA, a calcium chelating agent) it does not make an obstacle to observing qualitatively different oscillations in the voltage. The questions Morris and Lecar want to answer in [10] are if the non inactivation of the conductances is enough to produce this variety of behaviours, and if neglecting further conditions (which naturally occur) is acceptable and does not make the model inaccurate. The results show that the answer to both queries is positive.

3.1 The original system and a fast-slow reduction

In this section we are going to present the original Morris-Lecar system and then perform a fast-slow reduction using a theorem by Tikhonov: the aim is to get an equivalent expression (from a qualitative point of view) for the system which enables us to apply methods and theorems used on state planes. The ODE proposed in [10] is the following:

$$\begin{cases} I = C\dot{V} + g_L(V - V_L) + g_{\mathrm{Ca}}M(V - V_{\mathrm{Ca}}) + g_{\mathrm{K}}N(V - V_{\mathrm{K}}) \\ \dot{M} = \lambda_{\mathrm{M}}(V)[M_\infty(V) - M] \\ \dot{N} = \lambda_{\mathrm{N}}(V)[N_\infty(V) - N] \end{cases}$$

where I is the applied current, V is the voltage, M and N play a role analogue to m and n in the Hodgkin-Huxley model, representing the fraction of open Ca^{++} and K^+ channels, and take values in $[0, 1]$. The g_j are the conductances associated to leak ($j = L$), calcium ($j = \mathrm{Ca}$) or potassium ($j = \mathrm{K}$), and are assumed to be independent functions of voltage. V_j is the equilibrium potential, for $j \in \{L, \mathrm{K}, \mathrm{Ca}\}$. $\lambda_M(V)$ (resp. $\lambda_N(V)$) is the rate of opening of the Ca^{++} (resp. K^+) channels. $M_\infty(V), N_\infty(V)$ are the fractions of Ca^{++} and K^+ channels

open at steady state. The last four quantities are described by the following equations:

$$\lambda_M(V) = \bar{\lambda}_M \cosh \frac{V - V_1}{2V_2} \tag{3.1}$$

$$\lambda_N(V) = \bar{\lambda}_N \cosh \frac{V - V_3}{2V_4} \tag{3.2}$$

$$M_\infty(V) = \frac{1}{2}\left(1 + \tanh \frac{V - V_1}{V_2}\right) \tag{3.3}$$

$$N_\infty(V) = \frac{1}{2}\left(1 + \tanh \frac{V - V_3}{V_4}\right) \tag{3.4}$$

where $\bar{\lambda}_M$ and $\bar{\lambda}_N$ are the maximum rate constants for the opening of the Ca^{++} and K^+ channels, V_1, V_2, V_3, V_4 are parameters (whose values are to be determined experimentally).
The system we are going to analyse is actually a 2-dimensional reduction of the original model: we want to apply a theorem by Tikhonov[1].

Theorem 3.1.1 (Tikhonov)**.** *Consider the dynamical systems:*

$$\begin{cases} \dot{u}_i = f_i(t, u_i, v_j) & i = 1, \dots, p \\ \varepsilon_j \dot{v}_j = F_j(t, u_i, v_j) & j = 1, \dots, m \end{cases}$$

for $(u_i, v_j) \in D \times G \subseteq \mathbb{R}^p \times \mathbb{R}^m$*,and assume*

- $u_i(t_0) = u_{i0}$, $v_j(t_0) = v_{j0}$
- *the solution exists and is unique for the reduced system*

$$\begin{cases} \dot{u}_i = f_i(t, u_i, v_j) & i = 1, \dots, p \\ 0 = F_j(t, u_i, v_j) & j = 1, \dots, m \end{cases}$$

- $\varepsilon_j(\epsilon_0) \leq \epsilon_0$ *for some parameter* $\epsilon_0 > 0$*, and* $\lim_{\epsilon_0 \to 0} \varepsilon_j(\epsilon_0) = 0$
- ε_j *may be functions of other variables.*

Now, if there exist functions ψ_j *defined locally so that* $F_j(t, u_i, \psi_j(t, u_i)) = 0$ *for each* j*, and a positive real number* r_0 *such that*

$$F(t, u_i, v_j) := \sum_{j=1}^{m} [v_j - \psi_j(t, u_i)] F_j(t, u_i, v_j) < 0$$

if

$$0 < \sqrt{\sum_{j=1}^{m} [v_j - \psi_j(t, u_i)]^2} < r_0$$

we say that the root of the system is stable. Define the region of influence of the stable root to be the set of the initial values (t_0, u_{i0}, v_{j0}) *such that for all the* v_j *between* v_{j0} *and* $\psi(t_0, u_{i0})$ *it holds that* $\operatorname{sgn} F(t_0, u_{i0}, v_j) = \operatorname{sgn} F(t_0, u_{i0}, v_{j0})$.

[1] We use the formulation contained in [12].

Then for any initial point (t_0, u_{i0}, v_{j0}) *in the area of influence of the stable root* $v_j = \psi_j(t, u_i)$*, as* $\epsilon_0 \to 0$ *we have* $\{(t_0, u_i(t, \epsilon_0), v_j(t, \epsilon_0))\} \to \{t, \bar{u}_i(t), \bar{v}_j(t)\}$*, which is the solution of the degenerate system*

$$\begin{cases} \frac{d}{dt}\bar{u}_i = f_i(t, \bar{u}_i, \psi_j(t, \bar{u}_i)) & i = 1, \dots, p \\ \bar{v}_j = \psi_j(t, \bar{u}_i(t)) & j = 1, \dots, m \\ \bar{u}_i(t_0) = u_{i0} \end{cases}$$

uniformly for $t \geq t_1 > t_0$

Our aim is to approximate the solutions for the (V, M, N) system with solutions of the (V, N) reduced system, as these will retain the qualitative features of the trajectories of the complete system by Tikhonov's Theorem: the trajectories of the reduced system in fact tend to the ones of the whole system for arbitrarily large times. Morris and Lecar had already mentioned this possibility on page 201 of [10], stating that the the "Ca^{++} system is assumed to be so much faster than the K^+ system that g_{Ca} is instantaneously in steady state at all times [i.e., $M = M_\infty(V)$]". Set $\varepsilon = \lambda_M^{-1}$: then if $\epsilon_0 = \bar{\lambda}_M^{-1}$ we have that

$$\varepsilon(\epsilon_0) = \bar{\lambda}_M^{-1}\left(\cosh\frac{V - V_1}{2V_2}\right)^{-1} \leq \bar{\lambda}_m^{-1} = \epsilon_0$$

$$\lim_{\epsilon_0 \to 0} \varepsilon = \lim_{\epsilon_0 \to 0} \epsilon_0 \left(\cosh\frac{V - V_1}{2V_2}\right)^{-1} = 0 \qquad \forall V$$

The solution locally exists and is unique for the reduced system as well, since all the functions are locally Lipschitz and not dependent on the time. We can find the function ψ manipulating algebraically the equation involving $\dot{M}$, getting:

$$M(V, N, t) = \psi(V, N, t) = M_\infty(V) = \frac{1}{2}\left(1 + \tanh\frac{V - V_1}{V_2}\right)$$

and now the function F is

$$F(t, V, N, M) = -\lambda_M(V)(M - M_\infty(V))^2 < 0$$

for $r_0 = \infty$, as $\lambda_M(V) > 0$, $(M - M_\infty(V))^2 \geq 0$ always. In particular $\operatorname{sgn}(F) = -1$ on the whole of $\mathbb{R}^4$ (we consider time as a coordinate following the statement of the theorem), and this is enough to apply Tikhonov's theorem: given *any* initial value, for large values of $\lambda_M(V)$ (which are easy to attain, as this quantity has exponential growth as a function of V) we are reduced to the study the following system:

$$\begin{cases} I = C\dot{V} + g_L(V - V_L) + g_{Ca}M_\infty(V)(V - V_{Ca}) + g_K N(V - V_K) \\ \dot{N} = \lambda_N(V)(N_\infty(V) - N) \end{cases}$$

Notice that by symmetry we could follow the same process with N as fast variable, but as noted in [9] given the parameters M is faster than N, and hence gives a better approximation[2].

[2]In the same paper it is proved that V is the fastest variable, but as it is what one is interested in studying removing it would be a useless dimensional reduction.
To have further information and for a proof of the reduction see [7]

3.2 Study of the reduced system

The first thing to notice here is that the trajectories are bounded: the N-component can take values between 0 and 1 by hypothesis, but it is not immediate to see that we can bound V to be in a rectangle. Setting $\dot{V} \geq 0$ one sees that

$$\dot{V} \geq 0 \quad \Leftrightarrow \quad V \leq h(N, V)$$

where $h(N,V) = \frac{I+g_L V_L + g_{Ca} M_\infty(V) V_{Ca} + g_K N V_K}{g_L + g_{Ca} M_\infty(V) + g_K N}$. Considering h as a function of M and N, being it continuous on a compact set, h has a global maximum. This suffices to say that $\dot{V} \geq 0$ if and only if $V \leq \max_{[0,1]\times[0,1]} h(M,N)$. With the same calculations and the same application of Weierstrass theorem we infer that $\dot{V} \leq 0$ if and only if $V \geq \min_{[0,1]\times[0,1]} h(M,V)$. With the same estimates we gave in Section 2.3.1 we conclude that the $V-$coordinate is bounded to stay in a compact interval of $\mathbb{R}$. With some calculations one can show that the voltage satisfies the inequalities:

$$\frac{I + g_L V_L + g_K V_K}{g_L + g_K} = V_{min} \leq V \leq V_{max} = \frac{I + g_L V_L + g_{Ca} V_{Ca}}{g_L + g_{Ca}}$$

observing that for any value of the parameters $\nabla h \neq 0$ on $[0,1]^2$, that the functions can only either increase or decrease on the sides of the square (without critical points) and that V_K is the only negative quantity involved.
If the system has an unstable equilibrium in the area where trajectories are confined, by Theorem 2.3.4 we have existence of a limit cycle.
The nullclines have equations:

$$\begin{cases} N = \frac{I - g_{Ca} M_\infty(V)(V - V_{Ca}) - g_L(V - V_L)}{g_K(V - V_K)} & V\text{-nullcline} \\ N = \frac{1}{2}\left(1 + \tanh \frac{V - V_3}{V_4}\right) & N\text{-nullcline} \end{cases} \tag{3.5}$$

3.2.1 Bifurcation parameter: I

In this section we are going to follow the analysis by Morris and Lecar, from [10]. Let us fix values for all the parameters but I. From equation 3.5 it is evident that the system has at least one equilibrium: the $V-$nullcline tends to $-\frac{g_L}{g_K} < 0$ and $-\frac{g_{Ca}+g_L}{g_K} < 0$ at $\pm\infty$ respectively, and has a vertical asymptote at $V = V_K$, and the thesis descends by continuity of both the nullclines. With a graphical

V_L	-60 mV	C	20 μF/cm^2
V_K	-80 mV	V_1	-1.2 mV
V_{Ca}	120 mV	V_2	18 mV
g_L	2.0 mS/cm^2	V_3	2 mV
g_{Ca}	4.0 mS/cm^2	V_4	17.4mV
g_K	8.0 mS/cm^2	$\bar{\lambda}_N$	0.07 (ms)$^{-1}$

Table 3.1: Values for the parameters in this section, from [14].

study we can infer that the equilibrium is unique, and that its dynamical features depend on I: as we see in Figure 3.2, changes in I only affect the V-nullcline, and an increase in I in particular moves the equilibrium to the right, and the

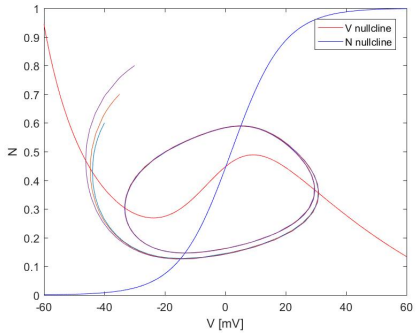

Figure 3.1: Intersection of the nullclines for $I = 150$, with limit cycle.

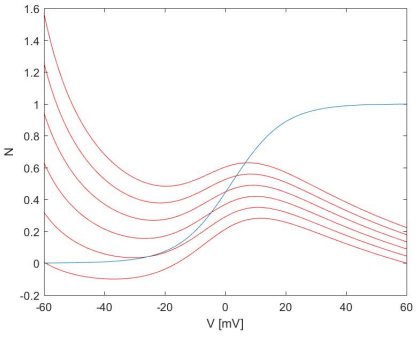

Figure 3.2: How the intersection points move as I is varied from 0 mA to 250 mA, with 50 mA between a curve and another.

derivative of the $V-$nullcline at the intersection can assume different signs.

Let (V_S, N_S) be the coordinates of the equilibrium. By linearisation of the system one gets that instability of the equilibrium is equivalent to the following conditions:

$$g_{Ca}\frac{d}{dV}M_\infty(V_S)(V_{Ca}-V_S) > \bar{g} + C\lambda_N(V_S) \tag{3.6}$$

$$g_{Ca}\frac{d}{dV}M_\infty(V_S)(V_{Ca}-V_S) < \bar{g} + g_K\frac{d}{dV}N_\infty(V_S)(V_S-V_K) \tag{3.7}$$

where $\bar{g} = g_L + g_K N_S + g_{Ca}M_\infty(V_S)$ is the equivalent conductance at the operating point. We want to show that there exists a value for I that causes (V_S, N_S) to satisfy the above inequalities, and one which prevents it. Given the geometric consequence of the variation in I this is enough to state that there is a bounded interval of $\mathbb{R}$ containing all the values of I for which the equilibrium is unstable: this follows from the observation that the right-hand side of 3.6 grows exponentially as a function of the voltage, while the left-hand side has a linear dependence times a bounded function.

Computing in MATLAB the coordinates of the equilibrium and the values of the expressions above, one sees that the inequalities hold for an applied current of $150\,\mu$A, but do not for a current of $0\,\mu$A. We can then perform calculations assuming different values for I, getting Table 3.2. We can see from Table 3.2

$I\,[\mu\text{A}]$	f_1	f_2	f_3
51.0	4.3941	4.2967	4.9683
51.1	4.4001	4.3536	5.0214
51.2	4.4063	4.4111	5.0753
51.3	4.4128	4.4700	5.1309
51.4	4.4194	4.5295	5.1874
51.5	4.4263	4.5897	5.2448
51.6	4.4335	4.6508	5.3036
51.7	4.4409	4.7130	5.3637
51.8	4.4485	4.7758	5.4248
51.9	4.4564	4.8394	5.4871
52.0	4.4645	4.9037	5.5505

Table 3.2: f_1 is right-hand side of (3.6), f_2 the left-hand side of the same inequality, f_3 is the right-hand side of (3.7).

that (3.7) is always verified, implying that the eigenvalues of the system always have the same sign. The trace of the Jacobian, however, changes sign for a value of the current somewhere between 51.1 μA and 51.2 μA: the eigenvalues simultaneously become of positive real part and the equilibrium loses stability, and by Poincaré-Bendixson a stable limit cycle is generated. We say that the system undergoes a **supercritical Andronov-Hopf bifurcation**.

3.2.2 Bifurcations in the plane (I, V_3)

In this section we are going to use the set of parameter in Table 3.1 except for V_3, following the analysis in [14]. A change in V_3 is reflected in a change of the slope at $V = 0$ for the N-nullcline, and in particular we see that for

certain values of V_3 there are three equilibrium points: a stable equilibrium, an unstable equilibrium and a saddle point in between the two. Now, increasing the

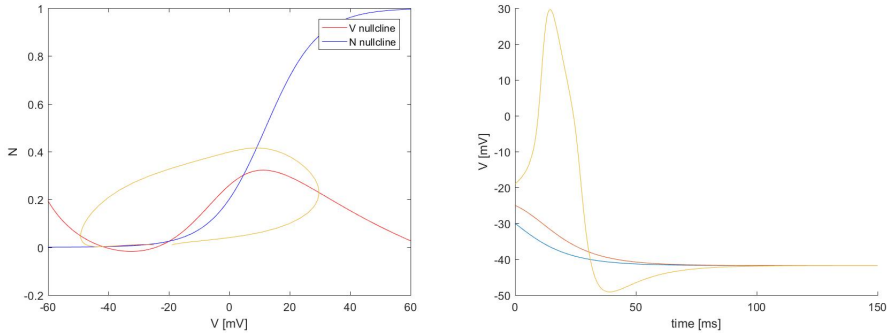

(a) (b)

Figure 3.3: For $I = 30\,\mu$A and $V_3 = 12$ mV we have three equilibria. The equilibrium to the left is stable, the middle one is a saddle point, the one to the right is unstable.

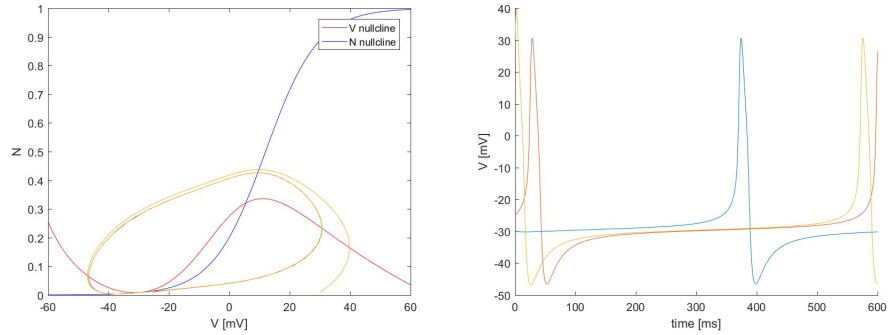

(a) (b)

Figure 3.4: $I = 39.8\,\mu$A, $V_3 = 12$ mV.

current I the V-nullcline moves upward, and the two left-most equilibria coalesce and disappear, and the system is said to undergo a **saddle-node bifurcation**, getting the same configuration as in the previous section with the generation of a stable limit cycle by Poincaré-Bendixson Theorem. We see this phenomenon in Figure 3.4 and 3.5. For different values of V_3 we have a completely different behaviour: starting with a small I the system has one stable equilibrium (see Figure 3.6), and increasing the current we create two equilibrium points, of which one is a saddle and the other is unstable. There is a small interval of values for I around $50.5\,\mu$A for which we have a bistable behaviour: two nested limit cycles are generated, the repelling inner one contains the stable equilibrium, the outer limit cycle is attracting: see Figure 3.7. The repelling limit cycle surrounding the equilibrium defines an area from which solution

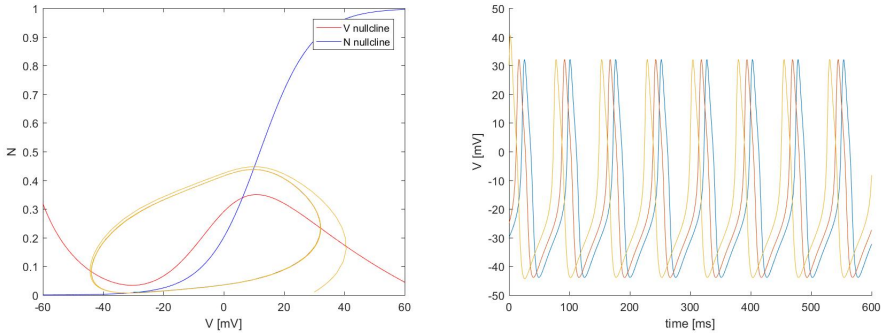

(a) (b)

Figure 3.5: $I = 50\,\mu$A, $V_3 = 12$ mV.

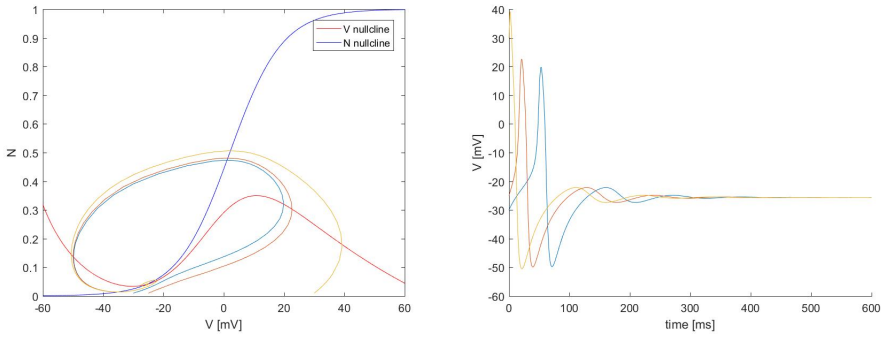

(a) (b)

Figure 3.6: I=50 μA, $V_3 = 2$ mV, there is only one stable equilibrium.

cannot escape, hence the oscillations are small and damped, given the attraction of the equilibrium. Outside the inner limit cycle solutions still tend to the outer limit cycle, and behave as above. If we increase I the inner repelling limit cycle

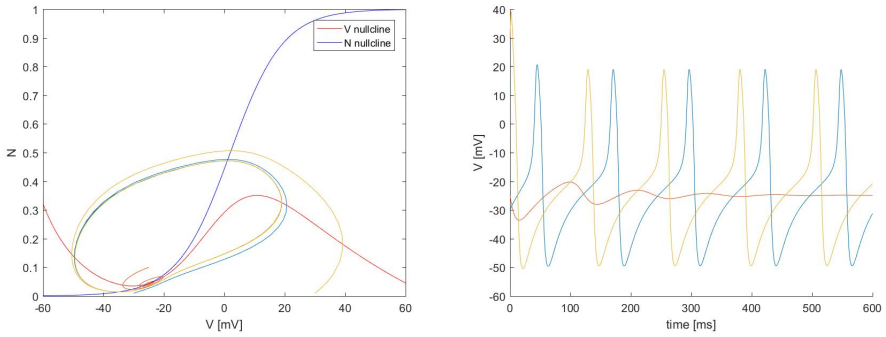

(a) (b)

Figure 3.7: $I = 50.5\,\mu$A, $V_3 = 2$ mV.

disappear, collapsing into the stable equilibrium and causing it to lose stabiity: we have a **subcritical Andronov-Hopf bifurcation**. Now, fix a small value

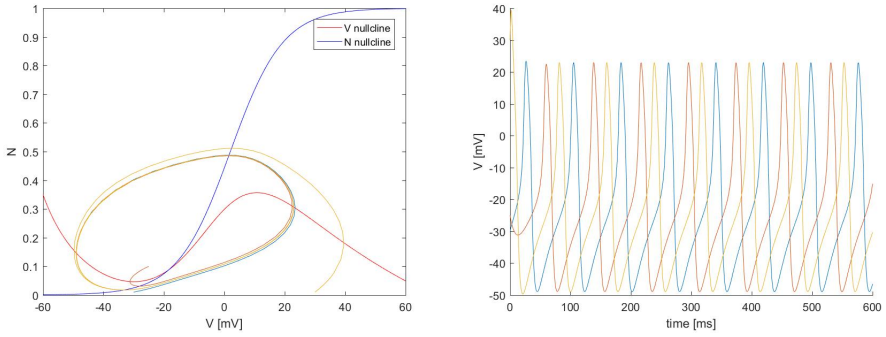

(a) (b)

Figure 3.8: $I = 55\,\mu$A, $V_3 = 2$ mV. The limit cycle has collapsed into the stable equilibrium, generating an unstable equilibrium.

for I, say $30\,\mu$A,and let V_3 vary. For a small V_3 we have again three equilibrium points from left to right: stable, saddle, unstable (Figure 3.9). If we increase V_3 the point to the right becomes stable and generates an unstable limit cycle surrounding it, and the system becomes bistable, see Figure 3.10. Increasing V_3 the unstable limit cycle around the right-most equilibrium gets closer and closer to the saddle, degenerating in a homoclinic loop when they touch. We can increase further V_3: the homoclinic loop vanishes and qualitatively we are left with the three equilibria we had at the first step.
Consider now the same values for V_3 we have just examined, and fix a larger I, say $I = 42\,\mu$A. For the first step $V_3 = 14.4$ mV we are in the same situation as

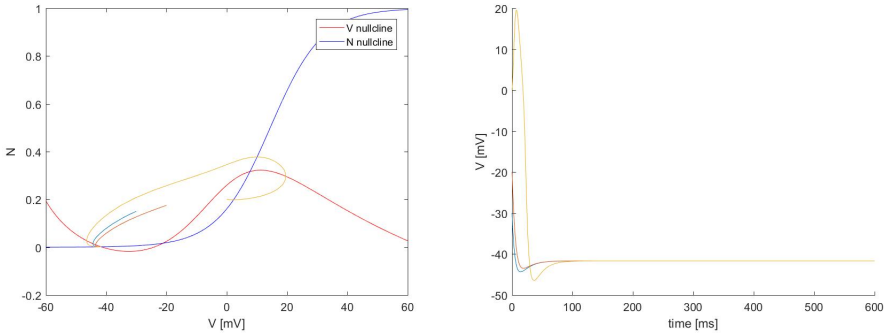

(a) (b)

Figure 3.9: $I = 30\,\mu\text{A}$, $V_3 = 14.4$ mV.

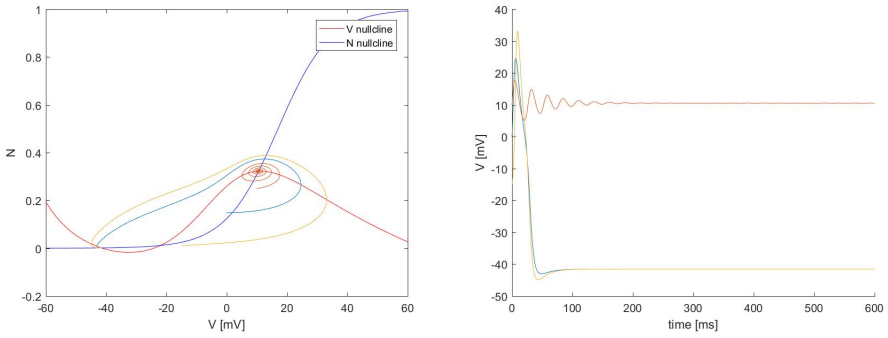

(a) (b)

Figure 3.10: $I = 30\,\mu\text{A}$, $V_3 = 17.0$ mV.

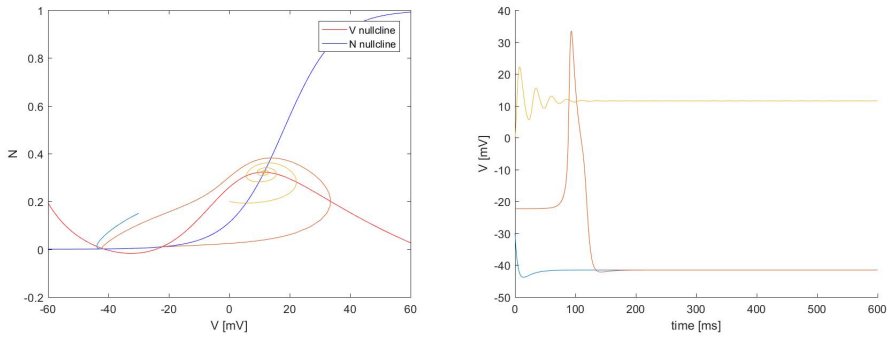

(a) (b)

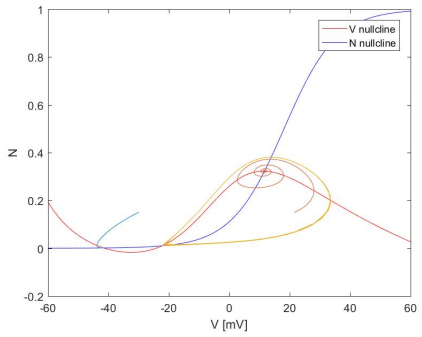

(c)

Figure 3.11: $I = 30\,\mu$A, $V_3 = 18.0$ mV. The homoclinic loop in c) was plotted integrating backwards in time starting from a point near the unstable equilibrium.

in Figure 3.5: we have a stable limit cycle and an unstable equilibrium. Now increase V_3 to 17 mV to find a subcritical Hopf bifurcation: the equilibrium becomes stable and generates an unstable limit cycle around it: there are now two limit cycles, one inside the other, as in Figure 3.7, but with a different position for the equilibrium: see Figure 3.12. Increase V_3: the two limit cycles

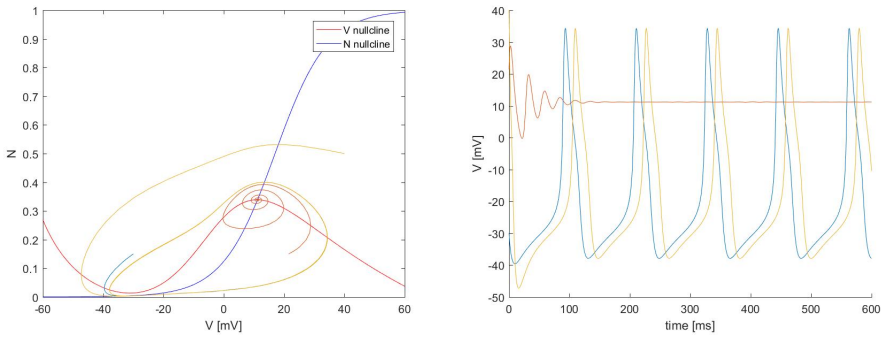

(a) (b)

Figure 3.12: $I = 42\,\mu$A, $V_3 = 17.0$ mV.

coalesce and disappear, leaving the system with just an attracting equilibrium. If

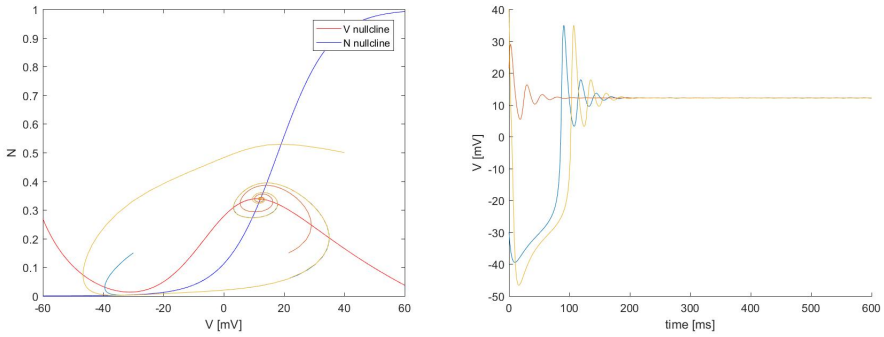

(a) (b)

Figure 3.13: $I = 42\,\mu$A, $V_3 = 18.0$ mV.

we fix V_3 at 4.1 mV and $I \approx 46.5\,\mu$A we are in an area where small variations in the current produce different kinds of bifurcations. In Figure 3.14 g_l indicates a set of values for the parameters for which we have a saddle-node bifurcation, h_k a set for which we have a Hopf bifurcation. H_i is a curve of homoclinic bifurcations and G_j one of tangent bifurcations. The shaded area is where three equilibria coexist, the striped one is where we have a limit cycle. Consider now the sequence of points Q to X. Decreasing I from Q go through a saddle-node bifurcation which does not generate any limit cycle, as it is given by the collapse of the saddle point with the source to the right, and the system still has an attracting equilibrium. Consider now Q: the system is in the usual configuration with three

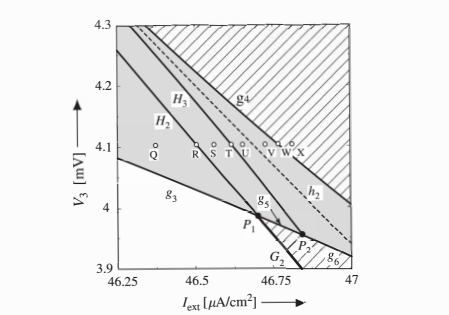

Figure 3.14: A portion of the bifurcation plane (I, V_3), from [14].

equilibria, from left to right: sink, saddle point, source. At R a homoclinic loop for the saddle point is generated: it encloses all the equilibria of the system, and with an increase of I degenerates into a limit cycle which still goes around all the equilibria (S). A further increase in the current generates another homoclinic loop for the saddle point, which then turns into an unstable limit cycle (U). The limit cycle shrinks and collapses onto the stable equilibrium, generating a source: subcritical Andronov-Hopf bifurcation (V). With an increase in I the left unstable equilibrium and the saddle point coalesce with a saddle-node bifurcation, and the system after this has a stable limit cycle with a source inside (X).

3.2.3 Bifurcation parameters: $(I, \bar{g}_{\mathbf{Ca}})$

In this section we are going to briefly report the different behaviours and bifurcations one may find while changing the values for the set of parameters $(I, \bar{g}_{\mathrm{Ca}})$: the bifurcation plane can be seen in Figure 3.16. The value fixed for V_3 is now 12 mV. Start from the top-left corner of the bifurcation diagram: for $g_{Ca} = 5.7$ mS/cm^2 and $I = 5\,\mu$A we are in a situation of bistability identical to the one in Figure 3.10, and an increase in I causes the system to undergo a similar homoclinic bifurcation (creation of the homoclinic loop for the saddle point encircling the unstable equilibrium). Increasing the current I we see a saddle node bifurcation, which annihilates the two left-most equilibria. Plotting the voltage over time we notice that we can arbitrarily delay the spike for a same initial point, setting the value of I closer and closer to the value of the saddle-node bifurcation. Starting with a lover g_{Ca}, say $g_{Ca} = 5.2$ mS/cm^2, with $I = 15\,\mu$A, one gets three equilibria. Increasing g_{Ca} one goes towards a subcritical Hopf bifurcation, to find the situation of previous step. Increasing g_{Ca} one finds the same Hopf bifurcation, with the unstable equilibrium gaining stability and generating an unstable limit cycle around itself. A further increase in the current leads the system to a saddle-node bifurcation with the destruction of the two equilibria at the left and the generation of a stable limit cycle encircling the unstable limit cycle. Increasing the current one has a tangent bifurcation: the two limit cycles collide and annihilate, leaving the system with only one stable equilibrium.
If we start with $g_{Ca} = 4$ mS/cm^2, the situation follows closely the previous step, without the first Hopf bifurcation: increasing I from 30 μA to 120 μA one starts

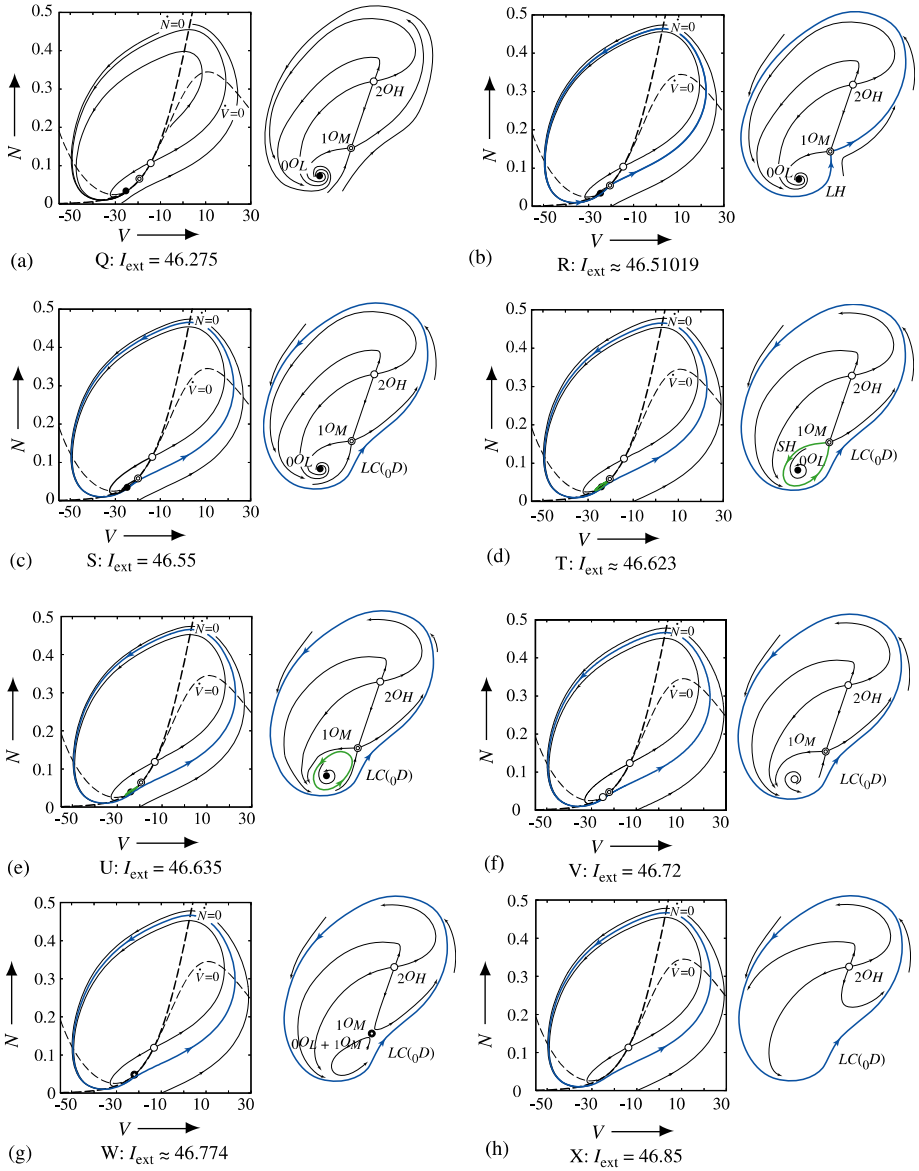

Figure 3.15: The different phase portraits for the points Q to X in 3.14. ${}_kO_l$ denotes an equilibrium, $k = 0$ if stable, $k = 1$ if saddle, $k = 2$ if unstable, l is used to distinguish them. ${}_kD_l$ indicates a limit cycle, $k = 0$ if stable, $k = 1$ if unstable. Image taken from [14].

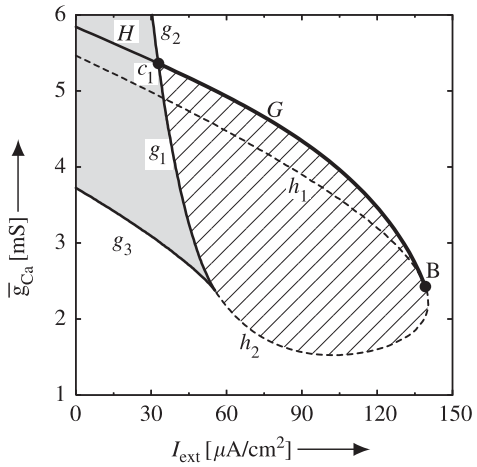

Figure 3.16: Bifurcation plane for the parameters $(I, \bar{g}_{\mathrm{Ca}})$, from [14].

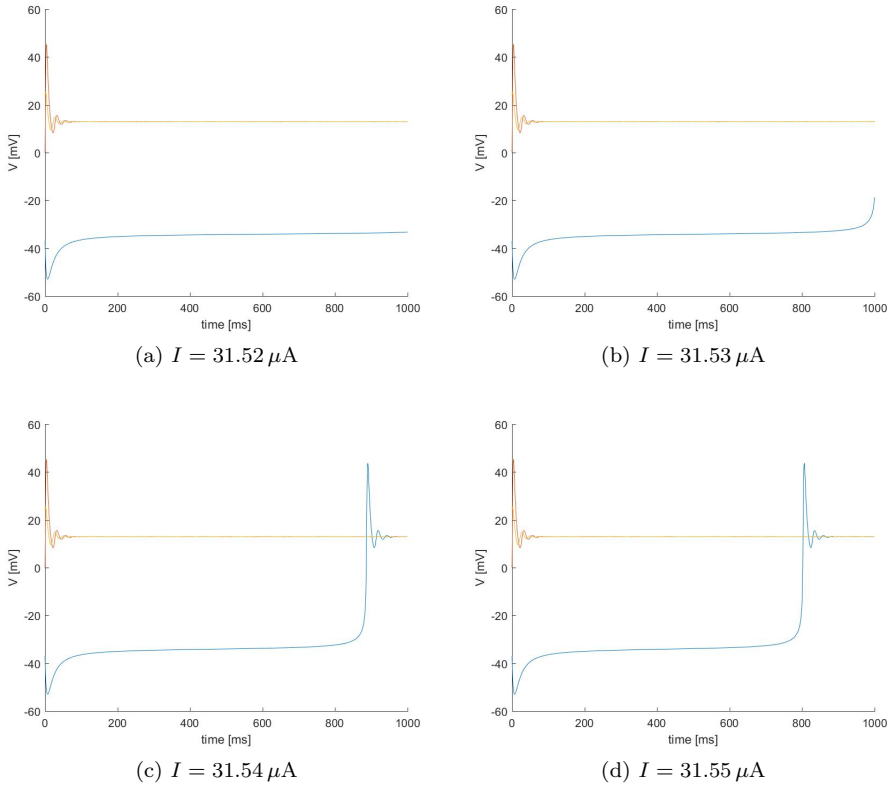

(a) $I = 31.52\,\mu$A

(b) $I = 31.53\,\mu$A

(c) $I = 31.54\,\mu$A

(d) $I = 31.55\,\mu$A

Figure 3.17: Delay of the spike for different values of I near the saddle-node bifurcation.

with three equilibria, loses the stable equilibria and the saddle in a saddle-node bifurcation which also generates a stable limit cycle by Poincaré-Bendixson; the unstable equilibrium then gains stability in a subcritical Andronov-Hopf bifurcation and generates an unstable limit cycle, which in the end annihilates with the outer stable limit cycle.
If we start with $g_{Ca} = 3$ mS/cm^2, $I = 30\,\mu$A, the system has one stable equilibrium, which is a global attractor. Increasing I one finds a saddle-node bifurcation, which generates a saddle and the unstable equilibrium on the right. Another saddle-node bifurcation annihilates the stable equilibrium and the saddle, with the generation of a stable limit cycle. With a subcritical Hopf bifurcation the equilibrium at the right becomes stable and generates an unstable limit cycle, which collapses with the outer stable limit cycle in a tangent bifurcation, and the system in the end has an attracting equilibrium.
The last case to consider is for an even smaller g_{Ca}: for $g_{Ca} = 2$ mS/cm^2, $I = 30\,\mu$A the system only has a stable equilibrium at the left. With an increase in I the equilibrium loses stability in a supercritical Andronov-Hopf bifurcation, and then the generated limit cycle for high values of I shrinks onto the equilibrium, which becomes stable again.

3.2.4 Bifurcation parameter: $(I, \bar{\lambda}_N)$

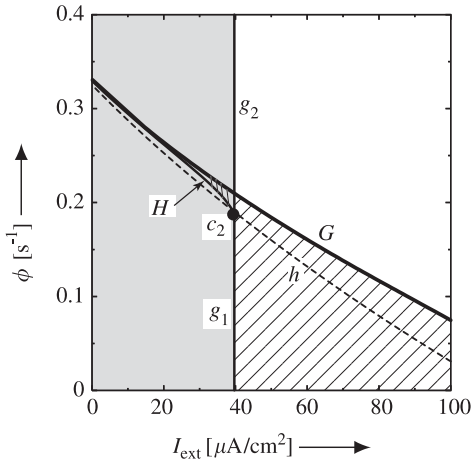

Figure 3.18: Bifurcation plane $(I, \bar{\lambda}_N)$, from [14]. In the picture, $\phi = \bar{\lambda}_N$.

Fix now g_{Ca} at the value in Table 3.1: we want to analyse the different possible behaviours of the system for different values of $\bar{\lambda}_N$. We see in Figure 3.18 that the behaviour is quite similar to the previous cases, except for the vertically-striped area: there we have a phenomenon of tristability, with a stable limit cycle and two stable equilibria. Fix $\bar{\lambda}_N = 0.2$ s^{-1}, and start with a current of $I = 20\,\mu$A: we are in the usual configuration with a sink, a saddle and a source. Increasing the current first we find a subcritical Andronov-Hopf bifurcation, where the source becomes a sink and generates an unstable limit cycle around itself. Increase the current further: a homoclinic loop for the saddle is generated in a homoclinic bifurcation, and this loop then becomes a stable limit cycle,

hence the tristability of the system. To see how tristability is generated, look at Figure 3.19. The phenomenon of tristability is then destroyed when with an increase in I the system undergoes a saddle-node bifurcation: the stable equilibrium and the saddle point touch and collapse. As we can see from Figure 3.18 then the system undergoes a tangent bifurcation, where the two limit cycles touch and collapse, leaving the system with the unstable equilibrium only.

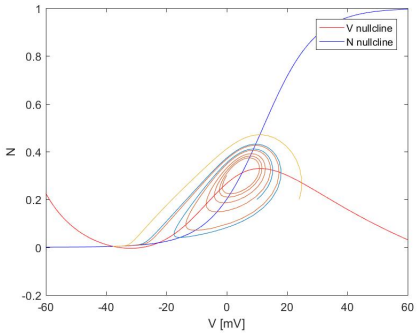

(a) $I = 35.0\,\mu$A

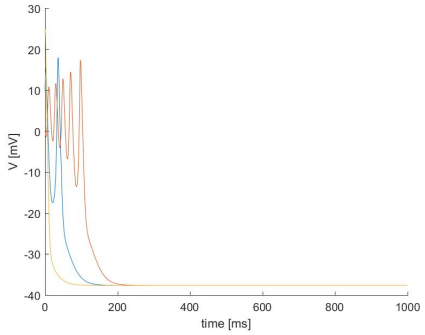

(b) $I = 35.0\,\mu$A

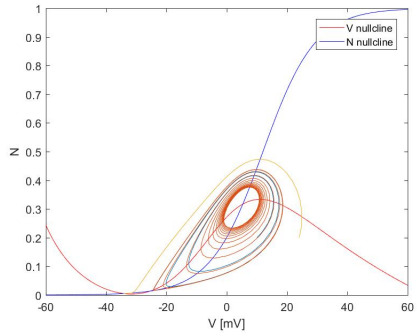

(c) $I = 38.0\,\mu$A

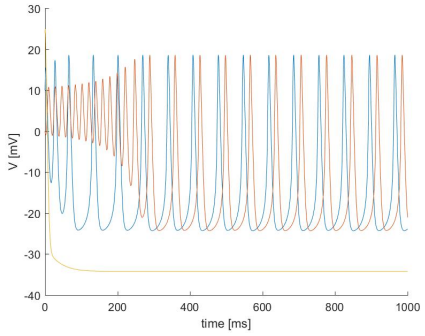

(d) $I = 38.0\,\mu$A

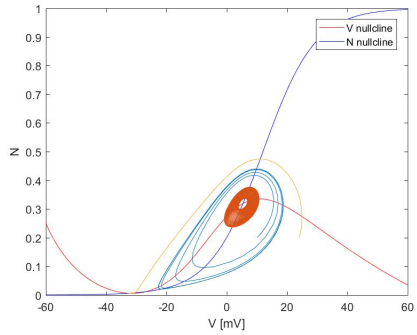

(e) $I = 39.0\,\mu$A

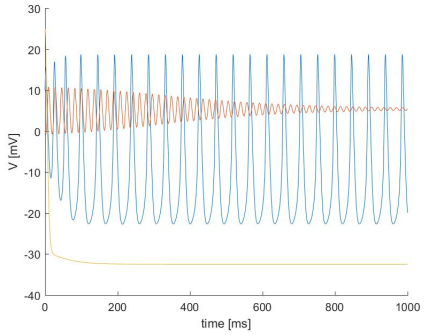

(f) $I = 39.0\,\mu$A

Figure 3.19: Generation of tristability varying I, for a fixed value of $\bar{\lambda}_N = 0.2$ s^{-1}.

3.2.5 Bifurcation parameters: (I, V_4)

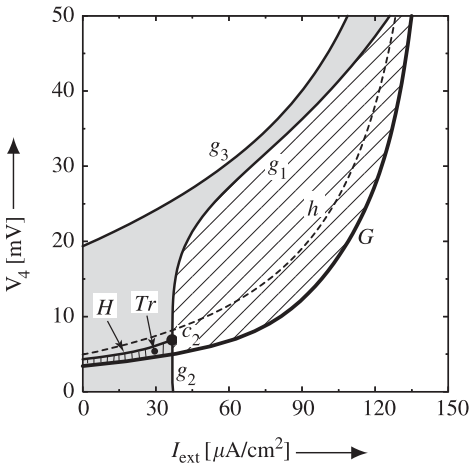

Figure 3.20: Bifurcation plane (I, V_4), from [14].

Here we will see how changes in (I, V_4) do not show any different mechanisms from what we saw above. In Figure 3.20 we find the bifurcation plane: in this case we have tristability as well, reached through a homoclinic bifurcation or a tangent bifurcation. The saddle-node bifurcation g_1 outside the area of tristability generates/annihilates the stable node and the saddle on a stable limit cycle, destroying/generating this.
Starting with coordinates $I = 30\,\mu$A, $V_4 = 10$ mV we are in the sink-saddle-source configuration. From here, increasing V_4 we go towards a saddle-node where the saddle and the source coalesce, leaving the system only with the stable equilibrium. Increasing current we go through a saddle-node bifurcation after which we are left with the unstable equilibrium surrounded by a limit cycle; the equilibrium then acquires stability in a Andronov-Hopf bifurcation, and the just generated limit cycle with a further increase in the current merges with the stable limit cycle on the outside in a tangent bifurcation: as a result the system has only one stable equilibrium at the right. From the initial point instead, if we decrease the voltage we first see an Andronov-Hopf bifurcation, with gain of stability for the rightmost equilibrium and generation of a limit cycle, then a homoclinic bifurcation which gives birth to a stable limit cycle and this way we have the tristability.

Bibliography

[1] N. Fenichel. "Geometric singular perturbation theory for ordinary differential equations". In: *J. Differential Equat.* 31 (1979).

[2] R. Fitzhugh. "Impulses and physiological states in theoretical models of nerve membrane". In: *Biophysical Journal* 1 (1961). DOI: 10.1.1.648.4753.

[3] R. Fitzhugh. "Mathematical models of threshold phenomena in the nerve membrane". In: *Bulletin of Mathematical Biophysics* 17 (1955).

[4] R. Fitzhugh. "Threshold and plateaus in the Hodgkin-Huxley nerve equations". In: *The Journal of General Physiology* (1960).

[5] A. L. Hodgkin and A. F. Huxley. "A quantitative description of membrane current and its application to conduction and excitation in nerve". In: *Journal of Physiology* 117.4 (1952). DOI: 10.1113/jphysiol.1952.sp004764.

[6] J. Keener and J. Sneyd. *Mathematical Physiology, 2 ed.* Springer, 2009. ISBN: 978-0387793887.

[7] I. Kobelevskiy. "Bifurcation analysis of a system of Morris-Lecar neurons with time delayed gap junctional coupling". In: (2008). URL: http://uwspace.uwaterloo.ca/handle/10012/3905.

[8] C. Kuehn. *Multiple Time Scale Dynamics*. Springer International Publishing, 2015. ISBN: 978-3319123165.

[9] H. Y. Li, Y. K. Wong, and W. L. Chan. "The asymptotic structure of the Morris–Lecar model". In: *Neurocomputing* 74 (2011).

[10] C. Morris and H. Lecar. "Voltage oscillations in the barnacle giant muscle fiber". In: *Biophysics Journal* 35 (1981).

[11] J. Nagumo, S. Arimoto, and S. Yoshizawa. "An active pulse transmission line simulating nerve axon". In: *Proceedings of the IRE* (1962).

[12] R. E. Plant and M. Kim. "On the mechanism underlying bursting in the aplypsia abdominal ganglion R15 cell". In: *Mathematical biosciences* 26 (1975).

[13] L. R. Squire et al. *Fundamental Neuroscience, Third Edition*. Academic Press, 2008. ISBN: 978-0123740199.

[14] K. Tsumoto et al. "Bifurcations in Morris-Lecar neuron model". In: *Neurocomputing* 69 (2006).